Metal Organic Frameworks as Emerging Carriers for Drug Delivery: A Review

[1]Bikash Meher, [2]Dr. Archanamayee Behera

[1]Research Scholar, [2]Assistant Professor

[1]Department of Chemistry, [1]Rajendra University, Balangir, Odisha,India

[1]safebikash@gmail.com, [2]archanabehera1990@gmail.com

Abstract: ***Metal-organic frameworks have rapidly gained popularity as a new type of material that combines organic linkers with metal ions. This huge family is becoming increasingly attractive for drug delivery due to their tunable porosity, chemical composition, size and form, and ease of surface functionalization. Over the last few decades, there has been an increasing interest in the development of tailored MOFs with regulated sizes for a range of biomedical applications. This article presents overall review and perspectives of MOFs-based drug delivery systems (DDSs). This article starting with the different strategies for synthesis of MOFs along with different factor that affect the synthesis. Then different general characterization techniques and nomenclature procedure also discuss. As the MOFs have wide range of application, we cover most important application like imaging, sensing, gas storage, separation catalysis, magnetism and biomedical application. After disusing the broadness of MOFs, we delegate our focus on different properties and functionalization for drug delivery. Procedures of drug loading on MOFs are also important so it is explained. Lastly, we classified the MOFs based on specific metal ion and organic ligand on account of drug delivery; with end of the section different therapeutic applications are explained.***

Keywords: ***MOFs, Bio-MOFs, drug loading, drug delivery system, synthesis method, characterization technique, bio- compatibility, Diseases therapy, bio-medical application.***

1. INTRODUCTION

Porous materials play an important role in our everyday lives. They've gotten a lot of press in a variety of domains, from structural materials to energy technologies, with applications in catalysis, adsorption/separation, biomedicine, and energy, among others. Traditional porous materials, such as zeolite, mesoporous silica, carbon, metal oxide, and polymer, are often entirely organic or inorganic. The majority of them are amorphous porous solids with uneven pores and indeterminate structures, making them unsuitable for studying structure-property connections. Zeolites, a type of crystalline porous solid with exceptional stability, periodic structure, and intrinsic acidity, have found widespread use in industrial adsorption and catalysis. Regulating the distribution of acidic sites is difficult, and the limited types of pore architectures are adverse aspects. As a result, scientific research into improved porous materials with well-defined, many, an easily customized structure for various purposes continues to be a hot topic. Porous materials are classified as microporous (pore diameters less than 2 nm), mesoporous (pore diameters between 2 and 50 nm), or macroporous (pore diameters greater than 50 nm) by the International Union of Pure and Applied Chemistry (IUPAC). Porosity can also be found in both organic and inorganic materials. Metal organic frameworks, a family of organic inorganic hybrid and crystalline porous materials have greatly enriched the realm of porous materials.

Over the last few decades, metal organic frameworks emerging its nobility on multiple branches of science. Till before February 14 ,1989 it was not even defined, after the work of Bernard F. Hoskins and Richard Robson [1] it's become diversified. It can be pondering as the combination of two major unit; a metal ion or cluster and an organic ligand. The organic ligand has capacity to donate multiple pair of electrons to the vacant orbital of the metal ion that leads to formation of multi-dimensional metal organic framework. MOF are the porous coordination polymers with crystalline structures. Up to until various organic ligand and metal ion were studied and more sufficient numbers of metal organic framework was produced in various research databases. On the basis of the ligand the metal organic framework may be classified as simple metal organic framework and Bio-

metal organic framework .In case of simple metal organic framework mainly organic linkers like BDC, BDC-NH_2,iso-phthalic acid ,benzene-1 ,4- di amine, pyrimidine etc. are involved .But in case of Bio-Metal organic framework instead of organic linker biomolecule are involved .Some of the organic biomolecule which are involved in metal organic framework are like nucleobases, amino acid, peptide ,protein , Porphyrins and metalloporphyrins , Cyclodextrin and other biomolecules

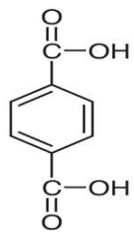

BDC

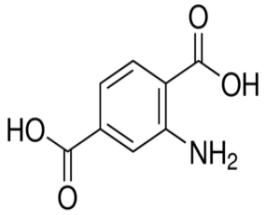

BDC-NH_2

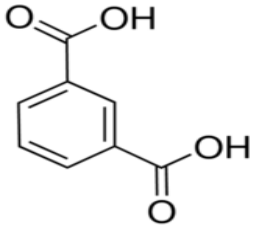

iso-phthalic acid

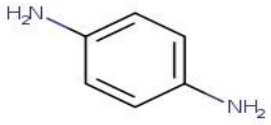

benzene-1 ,4- di amine

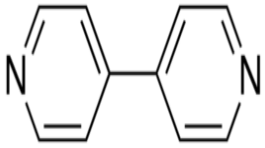

4, 4'-bipyridine

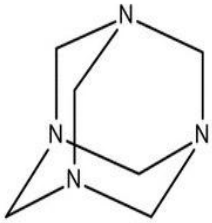

hexamethylene tetraamine

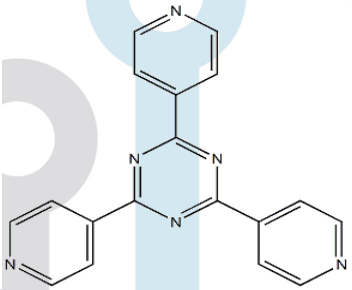

2 4 6-tris(4-pyridyl)-1 3 5-triazine

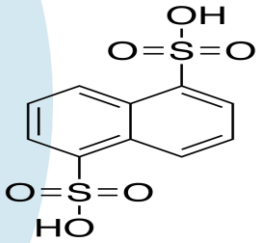

1 5-naphthalene disulfonic acid

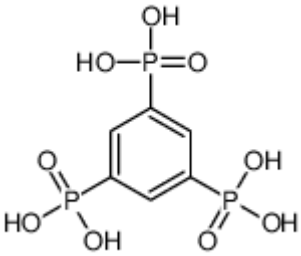

Benzene-1,3,5-triyltris(phosphonic acid)

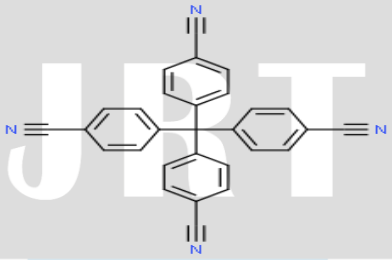

tetrakis(4-cyanophenyl)methane

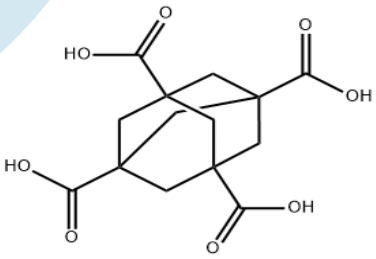

adamantanetetracarboxylic acid

Fig. 1.1 Examples of organic ligands for the preparation of MOFs

On the other hand, on the basis of structural features, it is classified in to rigid, flexible, open metal site and surface functionalized framework group. The rigid framework is utilized in sieving due to porous, stable and robust framework. The porosity helps to adsorption and desorption of gest molecule. While the flexible or dynamic framework affected by the external parameter such a temperature and pressure. The dynamic features exhibit breathing effect during absorption and desorption of gest molecule. Due to the breathing effect, there is a dynamic change of pore volume takes place. Other some flexible modes are swelling, linker rotation, and sub-network displacement. The open metal site frameworks have allowed design of well defied molecular absorption binding sites. The significance of this framework is on separation, gas absorption, single site catalysis and chromic sensor. Lastly the surface functionalized MOF which resulting due to the post synthetic grafting of selective functional ligands. These types of MOF have cellular transfection capability, bio compatibility, target cancer therapy, selective absorption, catalytic activity and molecular recognition.

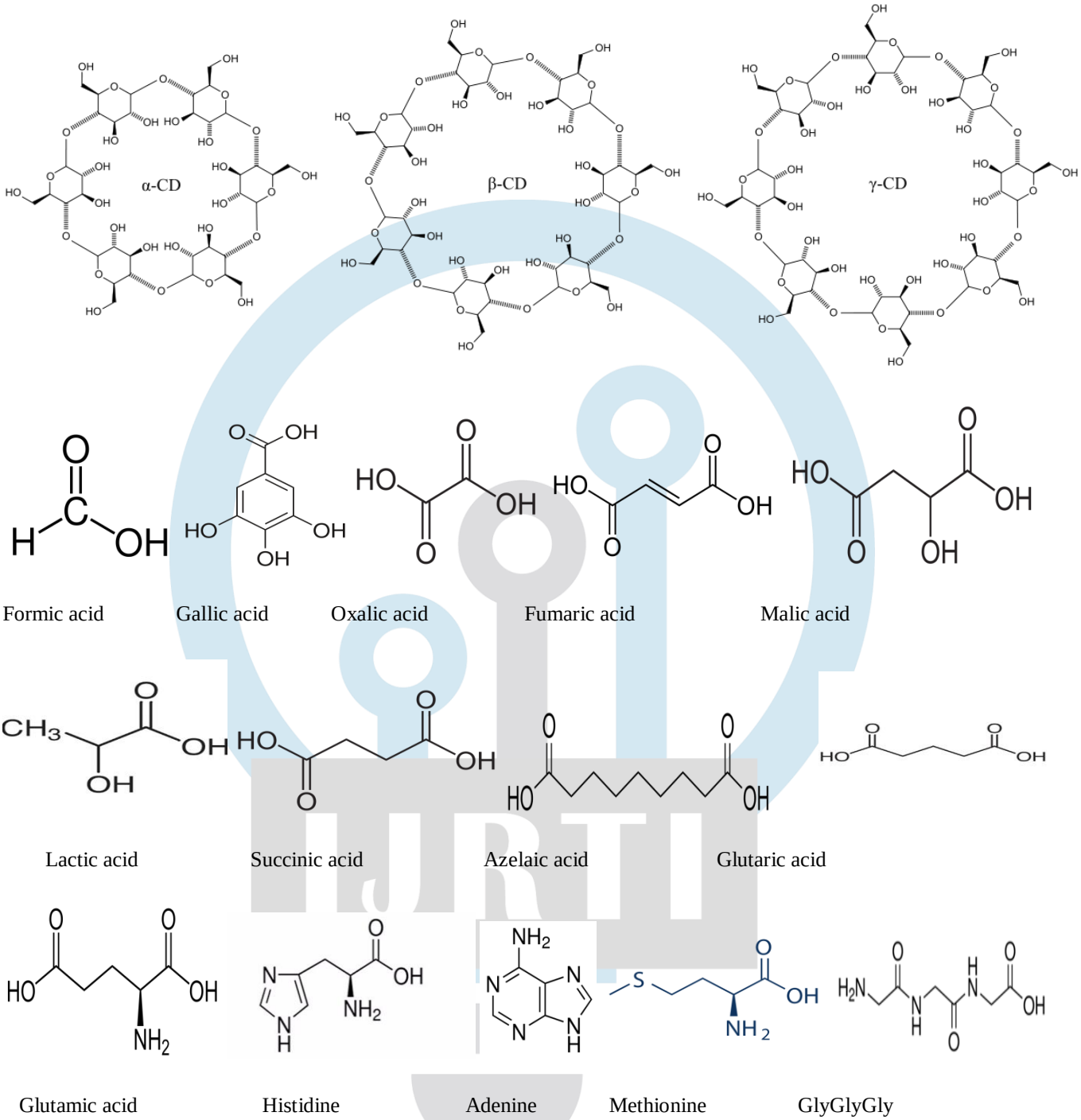

Fig. 1.2 Examples of organic linkers used for the synthesis of Bio-MOFs.

As initially we discussed that MOF is consist of two major component metal ion or cluster and organic ligand. But in structural aspects it consists of primary and secondary building units. Basically, in primary building unit metal ion act as linker to form a multidimensional polymeric MOF structure as in fig 1.3. In which metal ion such as some alkali metal, alkaline earth metal, rare earth metal and some transition metals are act as primary connector units with some precursor like nitrate, sulphate, oxide, acetate and chlorides of metal are used for synthesis rotes. However metal rods are used for electrochemical synthesis. For this organic ligand amine, nitrile, phosphate, sulfonate, carboxylate etc. are used. On the other hand in secondary building units instead of metal ion alone, Metal-oxygen-carbon clusters linked with organic linkers to form MOF. On initially modular synthesis method are employed to get the crystalline porous network. Now different method and technique are employed. Basically, there are two methods in which the MOF are synthesized that is conventional solvothermal and unconventional method, also in some alternative method it can synthesized.

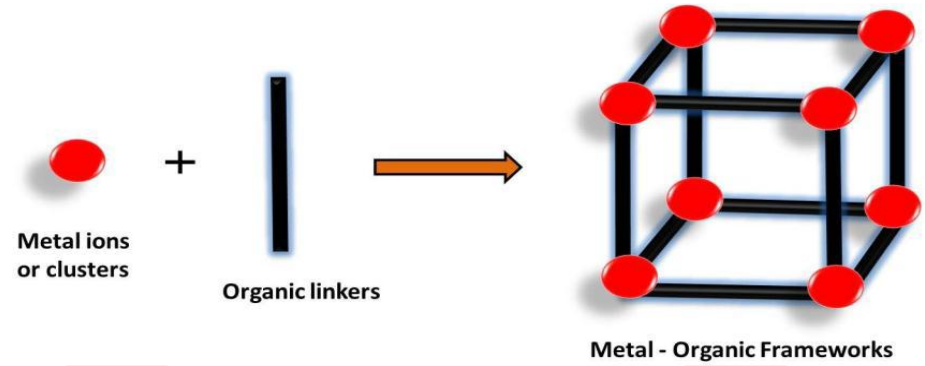

(a)

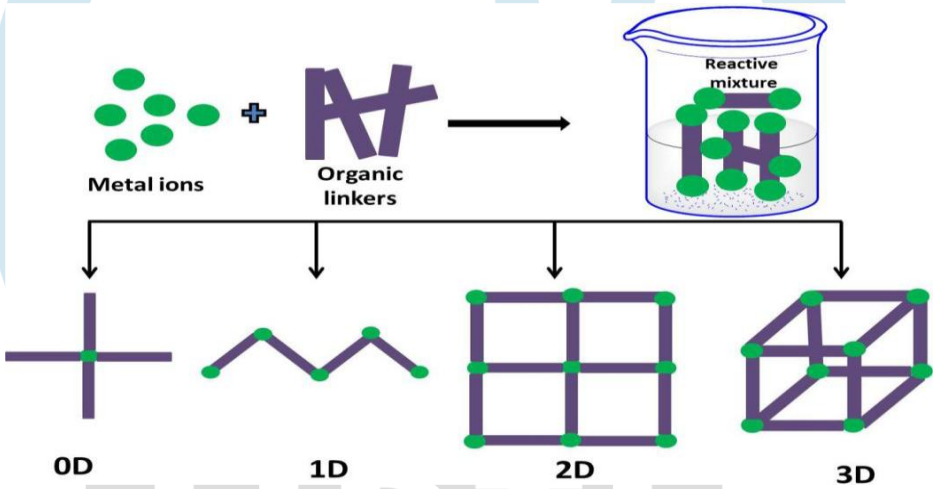

(b)

Fig.1.3 Schematic representation of the formation of MOFs (a) with different dimensionalities (1D, 2D and 3D) from the same PBUs (b).

The characteristic properties of the material such as; tunable surface area, ultrahigh porosity, flexibility, charge conductivity, hydrophobicity, thermal and chemical stability etc., gives the rich ground of application. The metal organic framework has incredible properties that may be used for imaging, gas storage, sensing, separation, catalysis, energy, biomedicine, and chemo analysis tool, among other things. Out of this diverse filed of application, bio medicinal utility as especially in the drug delivery system metal organic framework play a crucial role. Due to the tunable size and structure, modulable porosity and facial surface functionalization properties of MOFs make a fast-growing field in the drug delivery systems. To represent the MOFs structure and properties we take some illustrating figure as follow (Fig. 1.4, Fig. 1.5).

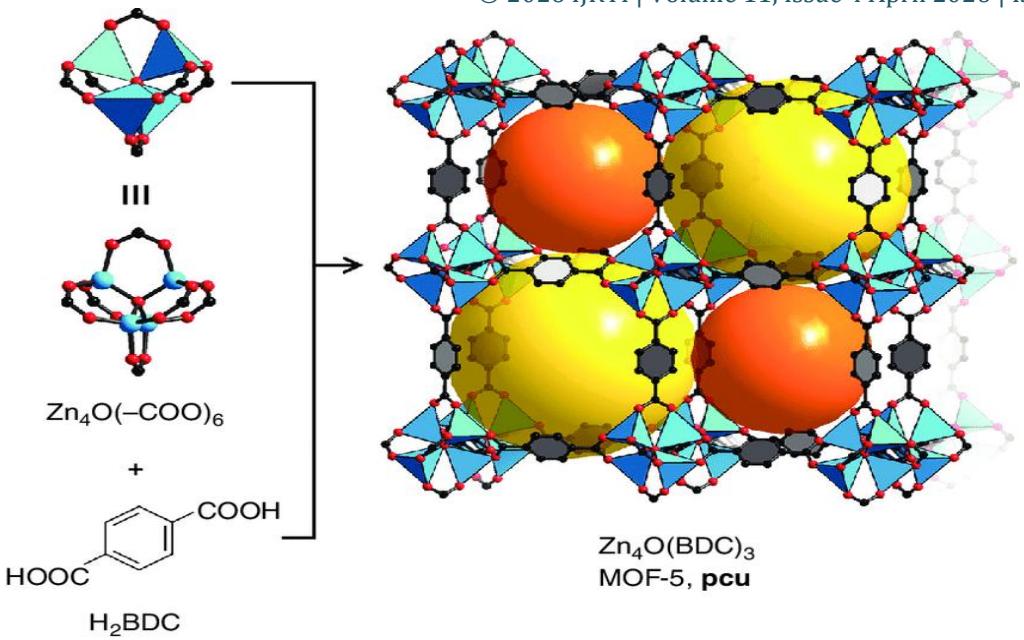

Fig 1.4. Single-crystal X-ray structure of MOF-5 constructed from $Zn_4O(–COO)_6$ SBUs, connected through BDC. The overall structure is composed of a large cavity (15.1 Å, yellow sphere) together with a smaller cavity (11.0 Å in diameter, orange sphere) in an alternating fashion. Hydrogen atoms are omitted for clarity. Color code: black, C; red, O; light blue polyhedra, Zn.

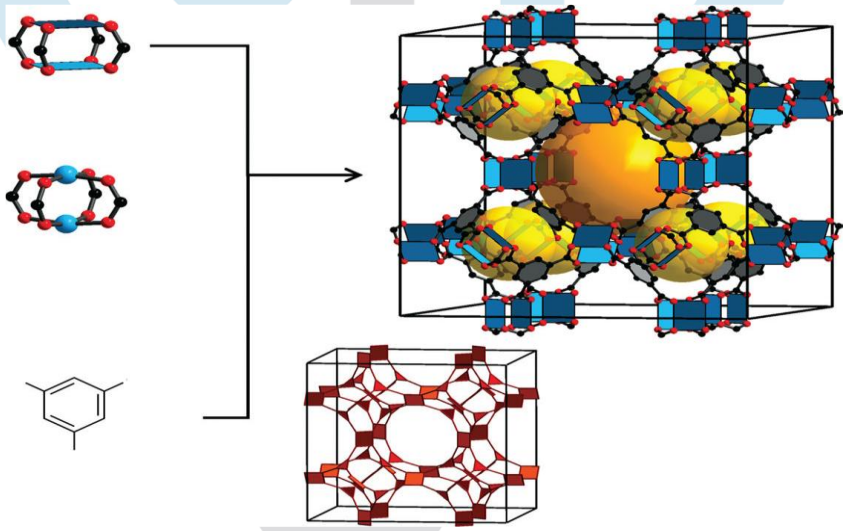

Fig 1.5 HKUST-1 Structure with synthesis by a combination of $Cu_2(–COO)_4$ and BTC. Hydrogen atoms and solvent molecules are omitted for clarity. Color code: black, C; red, O; blue, Cu. The yellow and orange balls represent the empty space in the framework.

MOFs have found applications in drug delivery systems (DDSs) in recent decades, and some unique designs and notable successes using MOFs for drug delivery have been realized. Similarly, papers on MOF-based DDSs depict a common trend over the last ten years. When compared to more traditional nanocarriers such as liposomes, polymers, quantum dots, and inorganic nanoparticles, the well-defined porous crystalline MOFs showed additional advantages, allowing researchers to avoid issues such as low drug loading, instability, systemic side effects, and toxicities. First and foremost, as porous materials with a large Brunauer-Emmett-Teller (BET) surface, MOFs have remarkable cargo loading capacities; a variety of cargos with varying physic-chemical properties, such as small drug molecules, peptides, and even bio macromolecules, can be loaded with efficiencies approaching 100%. Second, the porosities and compositions of MOFs can be tweaked by choosing the right building blocks and

metal ions to achieve certain physical and chemical features like biodegradability, drug loading efficiency, and controlled release. Furthermore, MOFs may be surface-modified easily employing predesigning or post- Furthermore; it is worth noting that altering the surfaces of MOFs rarely results in major changes in their physicochemical properties. Micro robots or surface functions are used in synthetic approaches to offer smart distribution. Indeed, due to cooperative interactions, coating materials can be readily adsorbed from aqueous media onto the MOFs surface with high yields and good stabilities or polymerized onto the surfaces. MOFs can also be coated with lipids or silica shells.

Finally, because MOFs' coordinative bonds have weak contacts, they are prone to disintegrate quickly in biological media, releasing their constitutive ligands. After completing the intended goal, this results in good biodegradability and biocompatibility. Last but not least, certain MOFs have intrinsic features that make them useful in the fight against cancer and infections. Specific Fe-based nano MOFs, for example, demonstrated: I) antibacterial capabilities, which helped combat intracellular infections in conjunction with their drug cargo and ii) participation in increasing radiation efficacy. These findings pave the path for the development of tailored nanoparticles (NPs) in which each component contributes to tumors treatment via radiotherapy or the treatment of severe illnesses. To put it another way, all of these qualities give MOFs a lot of promise in the field of DDSs.

In light of the expanding number of studies on MOFs over the last decades, several relevant reviews on the application of MOFs in biomedicine have been published in recent years on various issues such as DDSs for cancer treatment and cancer theranostics .MOF-based stimuli-responsive systems and MOF-composite materials for biological applications have been developed thanks to its tunability and ease of functionalization. Wang et al. [2] outlined the mechanisms of drug release in relation to endogenous stimuli (e.g., pH, glutathione, and enzyme) and exogenous stimuli (e.g., pH, glutathione, and enzyme) (e.g., temperature, light). Similarly, Cai *et al*. [3] divided MOF-based stimuli-responsive devices into single and multiple stimuli categories. On the other hand, Giliopoulos et al. [4] developed a number of polymer/MOF nanocomposites for drug delivery and imaging. Also published was a review of MOF composites and surface functionalization for nanomedicine in cancer therapy and diagnostics. Metal ions and bimolecular likers such as nucleobases, Cyclodextrin, amino acids, polypeptides, and others were also summarized and discussed in Biological MOFs (BioMOFs) for bio-applications. On the other hand, as drug delivery systems, MOFs were compared to other nanocarriers such as mesoporous silica nanoparticles and dendrimers.

This review, on the other hand, concentrates on MOF-based DDSs rather than MOF bio-applications. To begin, a classification of MOFs for DDSs will be offered, based on the type of constitutive metals and ligands used. The synthesis and characterization methodologies for MOFs and MOF-based DDSs are then summarized. Following that, three aspects of MOF-based DDS applications are catalogued. On the one hand, the functions of MOFs-based DDS in pharmaceutics, such as solubilization, enhanced stability, and sustained release, are discussed. Practical applications of MOF-based DDSs in the realm of diseases, on the other hand, are listed, including the treatment of infections, cancer, pulmonary and ophthalmic ailments, and so on. Simultaneously, the functionality of MOF-based DDSs for advanced applications is demonstrated. In addition, the bio pharmaceutics of MOFs and MOF-based DDSs is highlighted, which has received less attention in prior reviews. Finally, quality control and biosafety of MOF-based DDS, which are crucial for clinical and industrial applications, are discussed.

2. SYNTHESES OF MOFs

2.1 SYNTHETIC METHOD

There are several methods of synthesis method of MOFs developed until today. Non-solvothermal methods, such as direct precipitation and vapors diffusion synthesis, and solvothermal methods, such as microwave-assisted solvothermal synthesis, synthesis by reverse-phase micro-emulsions, electrochemical synthesis, dry-gel conversion methods, and preparation using a

microfluidics device, mechanochemical or sonochemical synthesis, layer by layer, step-by-step synthesis have all been used to synthesize all types of MOFs for drug delivery.

2.1.1 CONVENTIONAL SYNTHESIS

Conventional MOF synthesis usually refers to reactions that are carried out by heating at various temperatures, which is one of the most essential aspects in the synthesis of MOFs. Nonsolvothermal synthesis (temperatures below or near the boiling point) and solvothermal synthesis (temperatures above or near the boiling point) are two types of traditional synthesis (where reactions taking place above the boiling point).

2.1.1.1 NONSOLVOTHERAM SYNTHESIS

It can be further divided into those that take place at room temperature and those that take place at higher temperatures. Precipitation reactions with recrystallization or vapors diffusion synthesis, for example, have been documented. Some MOFs, such as HKUST-1, MOF-5, MOF-177, MOF-74, and ZIF-8 have been synthesized using the direct precipitation approach by simply combining the starting components at room temperature. Chemical and thermal stability were excellent in several of these MOFs, such as ZIF-8. The vapor diffusion approach was the first method for synthesizing CD-MOFs. Stoddard's group [5] created a variety of -CD-MOFs by mixing -CD with K^+, Rb^+, Cs^+, Na^+, or Sr^+. In some CD-MOF synthesis, a higher reaction temperature is also necessary to achieve good crystallinity and high yields. It was observed that changing the temperature from room temperature to 50 ℃ shortened the reaction time of -CD-MOFs synthesis from days to 6h.

2.1.1.2 SOLVOTHERAM SYNTHESIS

By boiling a mixture of methanol and water containing -CD and sodium oxalate at 160 ℃ for 3 days, a -CD-MOF was created. After heating at 160 ℃ for 4 days, Sha *et al.* [6] developed a unique -CD-MOF with a mixture of -CD and KOH. MOF-5 was synthesized at 105 ℃, which resulted in a significantly greater yield than those achieved at room temperature. In order to obtain MOFs in the laboratory, nonsolvothermal and solvothermal syntheses are limited. It's critical to create new synthetic methods for MOF manufacturing on a large scale. Ding *et al.* [7] described a novel CD-MOF manufacturing approach based on crystal transformation to industrialization, which increased productivity yield by a factor of a dozen when compared to previously published synthesis methods.

2.1.2 UNCONVENTIONAL OR MECHANOCHEMICAL SYNTHESIS

A mixture of metal salt and organic linker is grinded without the use of solvent in a mortar pestle or a ball mill, and then gently heated to evaporate any water or other volatile molecules created as by products in the reaction mixture. The mechanochemical method is the name given to this method. In this procedure, mechanical force is used to break intramolecular connections, which is then followed by a chemical reaction. Because no solvent is used, the process is recognized to be ecologically safe and can produce high yields of products. Short response durations, typically in the range of 10-60 minutes, can give quantitative quantities of tiny MOF particles. In many circumstances, metal oxides were favoured as a starting material over metal salts, resulting in merely water as a byproduct. Pichon *et al.* [8] were the first to disclose the synthesis of porous frameworks employing a mechanochemical technique in 2006. A comparison of solvothermal and mechanochemical approaches was used to explore a bipyridene-based covalent organic framework (COF), and it was discovered that only mechanochemically synthesised COF had proton conducting property. Liquid-assisted grinding (LAG) is a mechanochemical technique in which a little amount of solvent is injected. By enhancing the mobility of the reactants, adding a little amount of solvent to the reaction mixture speeds up the mechanochemical reactions.

2.1.3 ALTERNATIVE SYNTHESIS METHOD

In addition to these strategies, other options have been explored. Alternative methods can result in varying crystallization rates, particle sizes, size distributions, adsorption characteristics, and morphologies, all of which might affect the material's attributes. Diffusion of guest molecules in porous materials with varying particle sizes, for example, can have a direct impact on catalytic activity, adsorption, and separation capacity. The following are some of the most important alternate routes:

2.1.3.1 MICROWAVE ASSISTED SOLVOTHERMAL SYNTHESIS

Due to several potential advantages such as environmentally friendly quick synthesis, high yield, and morphology and size control, it has been frequently used for MOF synthesis under microwave assisted hydrothermal conditions. MIL-100 was the first MOF synthesised via microwave aided solvothermal synthesis. MIL-100 (Cr) microwaved at 220 °C for 4 hours had physicochemical attributes comparable to those synthesised at 220 °C for 4 days using conventional heating. MIL-100 (Fe) nanoparticles (NPs) with narrow particle size distribution, faceted shape, and high porosity were produced at 130 °C for 6 minutes. Microwave aided synthesis provided the best results in terms of high yields, small diameters (100 nm), and monodispersed NPs among the various MOF formation methods. In few minutes, "green" synthesis produced fluorine-free MIL-100 (Fe), paving the way for large-scale nano-MOFs for biomedical applications.Hf, Zr, Zn, and Ca based nanoMOFs for drug delivery were recently synthesised using microwave assisted solvothermal synthesis. Using the microwave-assisted approach, Liu *et al.* [9] were able to obtain -CD-MOFs in less than 10 minutes. Both micro and nanometer-sized crystals were generated by adjusting the reaction temperature, duration, and solvent ratios. Fast crystallization of HKUST-1, MIL-53 (Fe), MIL-101-NH_2 (Fe), ZIF-8, and MIL-100 were also discovered to be a method of choice.

2.1.3.2 SONOCHEMICAL SYNTHESIS

The sonochemical approach is a simple and ecologically efficient way to make MOFs quickly. When high-energy ultrasound interacts with liquids, bubbles develop and collapse in the solution, resulting in extremely high local temperatures of up to 5000 K and pressures of up to 1000 bar, a process known as acoustic cavitation. This results in extremely fast heating and cooling rates (>1010 K/s), which is beneficial to fine crystal formation. In an ultrasonic bath, HKUST-1 was created using a combination of DMF, ethanol, and water. After only 5 minutes of sonication, nanocrystalline NPs (10-40 nm) developed. Larger crystals (50200 nm) were obtained by increasing the sonication time, however further sonication resulted in crystal breakdown. MOF-5 (5-25 m), MOF-74 (Mn) (0.6 m), PCN-6 (4.5-6.0 m), IRMOF-9 (5-20 m), PCN-6 (1.5-2.0 m), and IRMOF-10 (5-20 m) were also prepared using the sonochemical approach. Ultrasound produced extremely small monodisperse MIL 88A nanoMOFs, but yields were modest.

2.1.3.3 ELECTROCHEMICAL SYNTHESIS

The production of 5MOF using an electrochemical method was initially described by BASF researchers. They developed new synthesis methods for MOFs using Zn, Cu, Mg, and Co as cathode materials and linkers such 1, 2, 3-H_3BTC, H_2BDC, 1, 3, 5-H_3BTC and H_2BDC-$(OH)_2$. Instead of metal salts reacting with dissolved linker molecules and a conducting salt in the reaction medium, electrochemical synthesis of MOF uses metal ions continually supplied through anodic dissolution as a metal supply. To avoid metal deposition on the cathode, protic solvents are utilized; however, H_2 is produced in the process. Normal batch reactions can also be done via the electrochemical approach. The electrochemical approach is also used to make MOFs with ionic liquids as linkers, such as [Zn $(MIm)_2$] and [$Zn(BIm)_2$]. Schlesinger et al. [10] synthesized HKUST-1 utilizing solvothermal, ambient pressure, and electrochemical approaches, comparing the effects of the various synthesis methods on the characteristics of the compound. It has been stated that the product generated using the electrochemical approach is of worse quality due to the insertion of linker molecules and/or conducting salt in the pores during crystallization.

2.1.3.4 LAYER BY LAYER SYNTHESIS

The layer-by-layer approach is used to create MOF thin films. The process is based on surface chemistry, in which a functionalized organic surface is immersed in metal ion and organic linker solutions consecutively. It was discovered that the orientation of thin films is determined by the order in which the reactants are added. Surface Plasmon Resonance (SPR) spectroscopy was used to investigate the kinetics of stepwise creation in this approach. The rate of formation of MOF films is influenced by two key factors: metal supply and surface termination. For substrates functionalized with diverse functional groups such as COOH, OH, highly oriented growth was found. Other synthesis routes have been adopted for MOF synthesis, such as chemical solution deposition (for the creation of thin film MOFs), post synthesis modification (where functional groups cannot be added during MOF synthesis), and ionthermal method (ionic liquids are employed as solvent). Fe-based MOF is generated via Fe-metallogels via gel degradation, according to Banerjee and coworkers [11]. Other MOF, on the other hand, have yet to be detected using this method.

2.2 FACTOR AFFECTING THE SYNTHESIS OF MOFs

2.2.1 SOLVENTS

MOF morphology is determined by the solvent system, which plays a crucial role in MOF synthesis. Solvents can act as space filling molecules or can coordinate with metal ions. Instead, they serve as a directing agent for the structure. Dimethyl formamide (DMF), diethyl formamide (DEF), dimethyl sulphoxide (DMSO), dimethyl acetamie (DMA), alcohols, acetone, acetonitrile, and other polar solvents are commonly utilized in MOF production. Depending on the solubility of the starting ingredients, a mixture of solvents may be utilized. Because of the polarity of the solvent utilized, as well as the solubility and protolysis properties of the organic linker, the reaction medium has an impact on the MOF formation process. It's also been noted that using different solvent systems in the same procedure produces MOF with varied morphologies. This could occur due to differences in the degree of deprotonation of organic linkers in various solvent systems. MOFs containing magnesium and PDC (3,5-pyridine dicarboxylic acid) with distinct crystal structures were produced under the same conditions using different solvent systems, according to Banerjee *et al* [12]. They discovered that the MOF network's dimensionality is determined by the solvent's capacity to coordinate with metal. When DMF/MeOH and EtOH/H_2O are used as solvents; H_2O has the strongest affinity for Mg, whilst EtOH and MeOH have no attraction for metal centres. Aside from structure, different solvent systems result in the synthesis of MOFs with varying pore sizes. Under comparable conditions, MOFs of cobalt and 4,4'-((5-carboxy-1,3-phenylene bis(oxy)) dibenzoic acid (H_3CPBDA) were produced using three different solvents: DMP, DMA, and DMF, resulting in pore diameters of76.84Å, 74.37Å and 72.76Å respectively. The size of the solvent molecule has been linked to the change in pore size caused by different solvents. The size of the molecules in the three solvents utilised varies as follows: DMP > DMA > DMF. In the same order, pore size decreases. Other researchers have found similar correlations.

2.2.2 EFFECT OF TEMPERATURE AND pH ON SYNTHESIS OF MOFs

The reaction medium's temperature and pH have a significant impact on MOF synthesis. At different pH levels, linkers can use different coordination modes. Furthermore, as the pH value rises, the degree of deprotonation of the linker rises as well. With rising pH, the Al^{3+} ion is coordinated with four, six, and eight carboxyl O-atoms, resulting in MIL-121 (pH = 1.4), MIL-118 (pH = 2), and MIL-120 (pH = 12.2). At higher pH values, an interpenetrated network is created, while at lower pH values, an uninterpenetrated network is formed. The colour of MOF compounds is also affected by the pH of the reaction media. Luoet *et al*[13] investigated three Co-MOF complexes: $[Co_2(L)(HBTC)_2(2\text{-}H_2O)(H_2O)_2]$, $[Co_2(L)(HBTC)_2(2\text{-}H_2O)(H_2O)_2]$, and $[Co_2(L)(HBTC)_2(2\text{-}H_2O)(H_2O)_2]$. $[Co_3(L)_2(BTC)_2]$, $3H_2O$ (1). $[Co_2(L)(BTC)(2\text{-}OH)(H_2O)_2]$, $4H_2O$ (2). By changing the pH value, $2H_2O$ (3) (L = 3,3',5,5' - tetra(1H-imidazol-1-yl)1,1' -biphenyl and BTC =1,3,5- benzenetricarboxylate) exhibits variable structure

and color. These three MOFs had diverse adsorption abilities in addition to structure and color. It's also been discovered that molecules with a higher dimension develop with a higher pH.

Another major element that impacts the characteristics of produced MOFs is the reaction temperature. Due to the increased solubility of reactants at high temperatures, greater crystallization occurs, resulting in the creation of big, high-quality crystals. The temperature of the reaction mixture influenced nucleation and crystal growth speeds. The temperature of the reaction media can also be changed to change the morphology of synthesised MOFs. Tm-succinate MOFs are made at different temperatures and have the same empirical formula but distinct morphologies, such as monoclinic and triclinic. Bernini et al. created two Ho-succinate MOFs and found that the MOFs prepared using the hydrothermal approach at a higher temperature were more thermally stable than the MOFs prepared at ambient temperature. Hydrothermal processes provide denser, less hydrated, and higher dimensional solids in addition to thermal stability.

2.3 FACTOR AFFECTING THE STABILITY OF MOFs

2.3.1 SURFACE ENGINEERING

MOF crystal formation can be influenced by "Coordination Modulation", which entails the introduction of monodentate ligands known as "Modulators" with the same functional group as the multidentate organic ligand already present. By modulating nucleation, modulators can accelerate or reduce crystal development, resulting in the creation of MOF crystals of various sizes. Modulators can be employed as "Capping agents" when they reduce crystal formation. As modulators/capping agents, sodium acetate, sodium formate, acetic acid, benzoic acid, n-dodecanoic acid,trifluoroacetic acid (TFA), pyridine, n-butyl amine, 1-methyl imidazole, polymers such as PVP, PEG, chitosan. The concentration of modulator has also been shown to affect the size and shape of MOF crystals. When lauric acid is utilised as a modulator in the microwave synthesis of HKUST-1, the crystal sizes vary from nano to micro scale. When a substantial amount of capping agent is employed, however, a new phase is formed. Modulators can improve the stability and specific properties of MOF crystals, such as molecule sensing, drug delivery, and so on. The imaging and anticancer properties of MOF111 coated with liposomes lipid have been investigated.

MOFs can also be altered by replacing a terminal ligand with a bridging ligand with a different function. Kitagava's research group effectively replaced the surface ligands of Zn-based MOFs $[Zn_2(1,4\text{-ndc})_2(dabco)]_n$ and $[Zn_2(1,4\text{-bdc})_2(dabco)]_n$ with boron dipyromethene, a fluorescent dye (BODIPY). Only the surface carboxylate ligands were altered in these MOFs, whereas the surface dabco ligands remained unchanged. Furthermore, because BODIPY is heavier than the initial carboxylate ligand, it only attaches to the surface. The influence of surface modification on the characteristics of ZIF–8 was proven by Liu et al [14]. When the surface ligand 2-methylimidazole is replaced with the more hydrophobic ligand 5, 6-dimethylbenzimidazol, it becomes more resistant to hydrolysis (DMBIM). Metal cation exchange in MOFs has been challenging to manage, in contrast to linker ligand exchange, because it can result in the creation of a Core-shell structure [15]. By adding Zn crystals to a solution of $CuSO_4.5H_2O$, 1,4-ndc, and dabco, Kitagawa and colleagues reported the core shell hybrid of Cu-MOF $[Cu_2(1,4\text{-ndc})_2(dabco)]_n$ produced on Zn similar $[Zn_2(1,4\text{-ndc})_2(dabco)]_n$. The development of green crystals on the Zn framework surface verifies the production of Cu-MOF [16].

2.4 NOMENCLEATRE

Due to a lack of widely accepted names, several attempts have been made to designate these novel hybrid materials, and parallel designations exist for related materials. The most typical examples are as follows: ZeoliticImidazolate Framework (ZIF), Metal peptide framework (MPF), Metal Azolate Frameworks (MAF), mesoporous Metal-Organic Framework (meso- MOF) and bio-MOF or MBioF - metal-biomolecule framework, are porous coordination polymer (PCP), porous coordination network (PCN), microporous coordination polymer (MCP), Zeolite-like Metal-organic Framework (ZMOF) etc.

2.4.1 ACRONIM OF THE LABORATORY WHERE THE MATERIAL WAS PREPARED

MOFs were given names based on the custom of naming novel compounds after laboratories or institutions. For example, in the series of MILs – Materials Institute Lavoisier, HKUST – Hong Kong University of Science and Technology, SNU – Seoul National University, South Korea, JUC – Jilin University China, CUK – Cambridge University- KRICT, POST – Pohang University of Science and Technology, South Korea, and so on, researchers used an acronym of the laboratory/institution where the material was created to name.

2.4.2 BASED ON THE STRUCTURE OF MOFs NET

MOFs are also given names based on their organization within the framework. O'Keeffe and colleagues, for example, proposed a systematic nomenclature for classifying known structures [17]. To designate a three-dimensional (3D) MOF network with a specific topology, a three-letter symbol, such as "dia", "cub", etc., or its extension (pcu-a", "cub-d", etc.) has been used. This approach allows researchers to describe and comprehend the internal structure of MOFs, as well as design and synthesis novel MOFs [18].

3. GENERAL CHARACTERISATION TECHNIQUES FOR MOFs

The materials were analyzed using a variety of characterization techniques, which are listed below.

3.1 POWDER X-RAY DIFFRACTION

X-ray diffraction (XRD) is an important method for determining the exact stoichiometry and structure of substances. Single crystal X-ray diffraction offers precise information about crystalline substances such as unit cell dimension, bond length, bond angle, and site-ordering features, whereas powder X-ray diffraction is beneficial for evaluating crystal cell parameters and material crystallinity. This research can be used to determine parameters such as crystallite size, phase composition and defect structures, strain state, and so on. It's also useful for determining the arrangement of atoms in amorphous materials and determining the thickness of thin films [19]. It is a non-destructive experiment because the substance is not harmed. A beam of monochromatic X-rays strikes crystals and is diffracted in many distinct directions due to their interaction with atomic electrons in X-ray diffraction. Interference occurs when X-rays dispersed from different sections of a crystal collide. Miller indices h, k, and l, which describe the lattice planes, must be aligned at Bragg's angle for constructive interference to occur.

$$n\lambda = 2\, d_{hkl} \sin\theta$$

Where is the incident light wavelength λ, d is the spacing between the layers, and θ is the scattered angle. Because of the spatial orientations of the Miller planes, each material has its own diffraction pattern, and each PXRD pattern resembles a specific sample. The Expert an analytical, JSM-6510 was used with Cu Kα radiation and a Gemonochromator to record unique X-ray diffraction patterns of MOFs. At room temperature, data was captured at a scanning rate of 2° per minute spanning the range 3° to 80°.

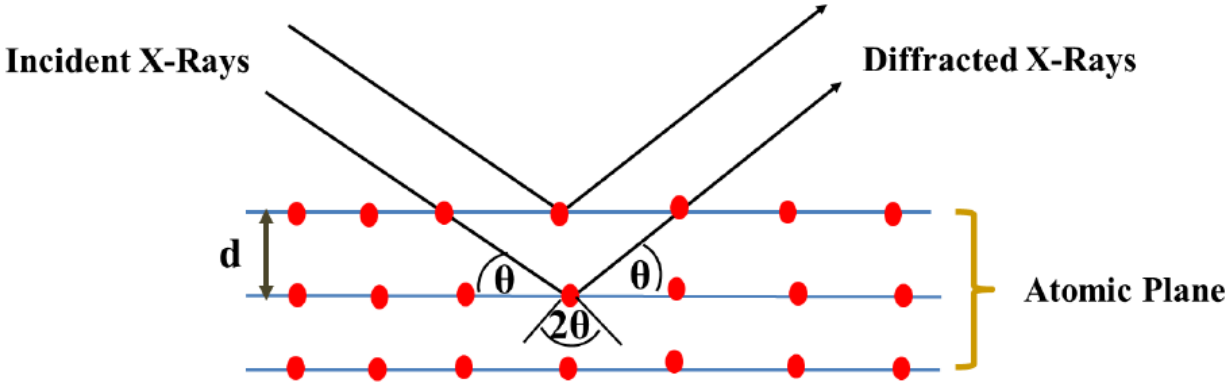

Fig 3.1 Bragg's law of diffraction

3.2 UV-VISIBLE AND IR SPECTRA MEASUREMENT

Reflectance, transmittance, and absorption are the processes that occur when light travels through any materials in a typical electromagnetic radiation, and these phenomena are detected using a spectrophotometer. When a monochromatic light beam strikes a substance, some of the light is absorbed by the color material and the remainder is transmitted. Despite the fact that all of the activities occur at the same time, measuring optical absorption is a standard procedure used by academics to better understand material behavior. UV-Vis spectrophotometer is used to study optical absorptions in the UV-VIS spectrum. The following equation is used to calculate incident light absorption:

$$I = I_0 e^{-\alpha t}$$

Where I= intensity of transmitted light, I_0 = intensity of incident light, t=thickness of the light absorbing material.

The photometer is used to measure the reflected light in most cases. The optical reflectance of MOF samples was evaluated using a UV-Visible and IR spectrophotometer device in the 200-800 nm range. We used a Thermo Scientific Orion Aqua Mate 8000 UV-Vis spectrophotometer with a 10 mm optical-path quartz cell at room temperature to assess dye adsorption, drug loading capacity in MOFs, and in-situ catalytic reduction of nitro to amino compounds. Using a UV-Visible and IR spectrophotometer with an integrating spherical sample holder, the UV-Visible disused reflectance spectra of solid MOF samples were examined.

3.3 SCANNING ELECTRON MICROSCOPE (SEM)

The scanning electron microscope is a useful tool for studying the microstructure of nanomaterials. Scanning Electron Microscopy's core concept is to illuminate a sample with a high-energy electron and quantify the relative phase and momentum of the reflected (back scattered) and expelled (secondary) electrons. The main electrons interact with the sample's surface electrons to collect data on the elemental makeup and surface properties. Depending on the surface shape and atomic electronic distributions of the sample, multiple deflections occur at various angles. Higher atomic number specimens deflect a greater amount of electrons, allowing the atomic composition of the samples to be determined.

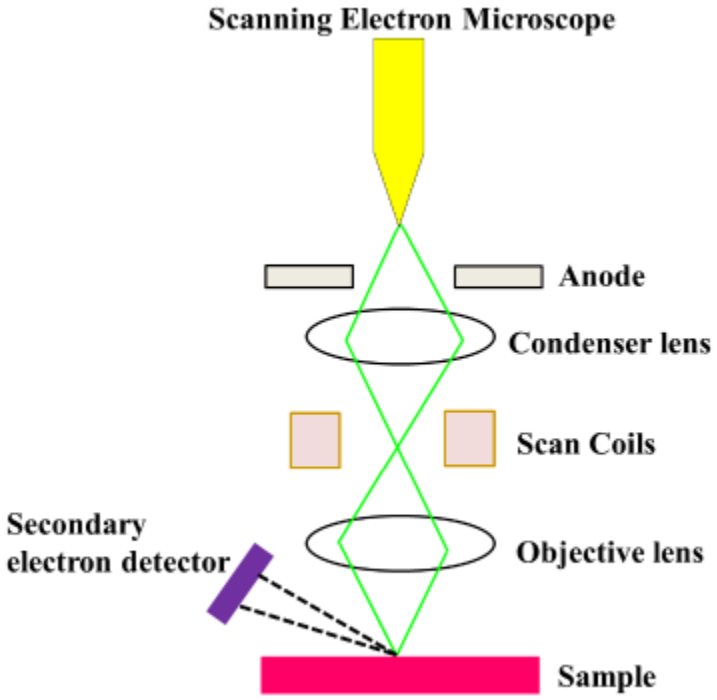

Fig-3.2 Schematic diagram of SEM

The type of the source/primary electron determines the intensity of back scattered/dislodged electrons. The information contained in the signals from ejected/secondary electrons of the samples includes exterior morphology (texture), orientation, and crystalline structure of the specimen. The SEM's high-energy source electrons interact with the samples' electronic structure and decelerate as they penetrate further into the sample. Diffracted backscattered electrons (BSE) are backscattered electrons that are frequently diffracted (DBSE). Secondary electrons, as well as BSE and DBSE, are used to assess sample orientations and crystal structures [20]. A schematic detail of SEM is shown in Fig. 3.2

MOF samples with surface exposure ranging from 5 microns to 1 cm were used in this study. The MOF sample was dissolved in methanol solution to make the specimen film for the experiment. For our investigations, magnifications ranging from 20X to 30,000X were used. To produce a satisfactory image of the specimen, the samples were scanned with a sufficient scanning period. 1mg of nano MOFs/materials were combined in 1 mL of methanol, and the solution was agitated with a vortex to ensure a homogenous suspension, as is customary in sample preparation for SEM. A homogeneous sample solution of around 10 micro liters was pipette out and dropped onto Si wafers/glass. The sample was dried until the entire methanol had evaporated.

3.4 FOURIER TRANSFORM INFRARED SPECTROSCOPY

The use of an infrared (IR) spectroscope to characterize samples fits into the current research since it provides information on the interactions of the sample (MOFs) with guest molecules (adsorbents) by modulating the vibration frequencies of the molecules' chemical bonds. Structurally sensitive spectroscopic techniques and IR characterization investigations are used to study the structure and a prospective change in the structure that could impact the structure-function relationship dramatically. In IR spectroscopy, a photon is absorbed by the material, and transitions between vibration states occur, whereas in Raman characterization, photon scattering is based on electronic polarization and is controlled by vibration motions. The molecular interaction between adsorbents and MOFs can be elucidated using these vibration approaches. (I) Raman active (a) symmetric stretching/bending modes (ii) IR active (a) symmetric stretching/bending modes are the usual vibration modes for molecules. The basic vibrational modes of this linear molecule will be disrupted once the guest molecule is adsorbed in MOFs, impacting the IR and Raman active modes. As a result, in practically all scientific analyses, IR is regarded as a simple and strong technique.

The analysis by IR spectroscopy involves an absorption law,

$$\log (I_o/I_t) = \alpha\, c l$$

Where α = absorption coefficient, l = path length, c = concentration of the sample which is analyzed, I_o= incident and I_t = transmitted light

In this study, the samples were analyzed for the FT-IR spectra of MOF using spectrophotometer (Thermo Fisher Nicolet iS5) with ID3 ATR sample holder. All the samples were characterized in the wavelength range of 4000 cm^{-1} to 400 cm^{-1}, but specific wavelength range were considered owing to the vibration frequencies of the MOFs, and MOF-adsorbent interactions.

3.5 THERMAL GRAVIMATRIC ANALYSIS

The thermal degradation process of porous materials was studied using a thermo gravimetric analyzer (TGA) throughout a temperature range of 300-900 K with a temperature rise of 0.5 percent. The purpose of this experiment is to investigate how well MOFs and other porous samples hold together. The thermal relaxation method is used to measure multiple crystals with a typical mass of 5-10 mg, as described below. A sample is analyzed for its dependability, material composition, and time or temperature in a conventional Thermogravimetry (TG) procedure. Single crystals, in general, are the finest form of a material and are required for determining the thermal parameters of adsorption and desorption processes. The thermogravimetry method of determining the atomic composition of a material does not require a significant sample mass (1-3 mg), hence it is simple to use. The measurements described in this paper were taken with a Hitachi STA-7200 commercial thermal decomposition analyzer with a temperature range of 273 to 1000 °C. The TGA option's software automatically fits the thermal pulse, solves for the characteristic time, and displays the user's weight loss. Prior to the sample, the contribution from the platform is measured and then subtracted. A schematic of a typical sample mount, as well as the apparatus used in this work, is shown in Fig.3.3.

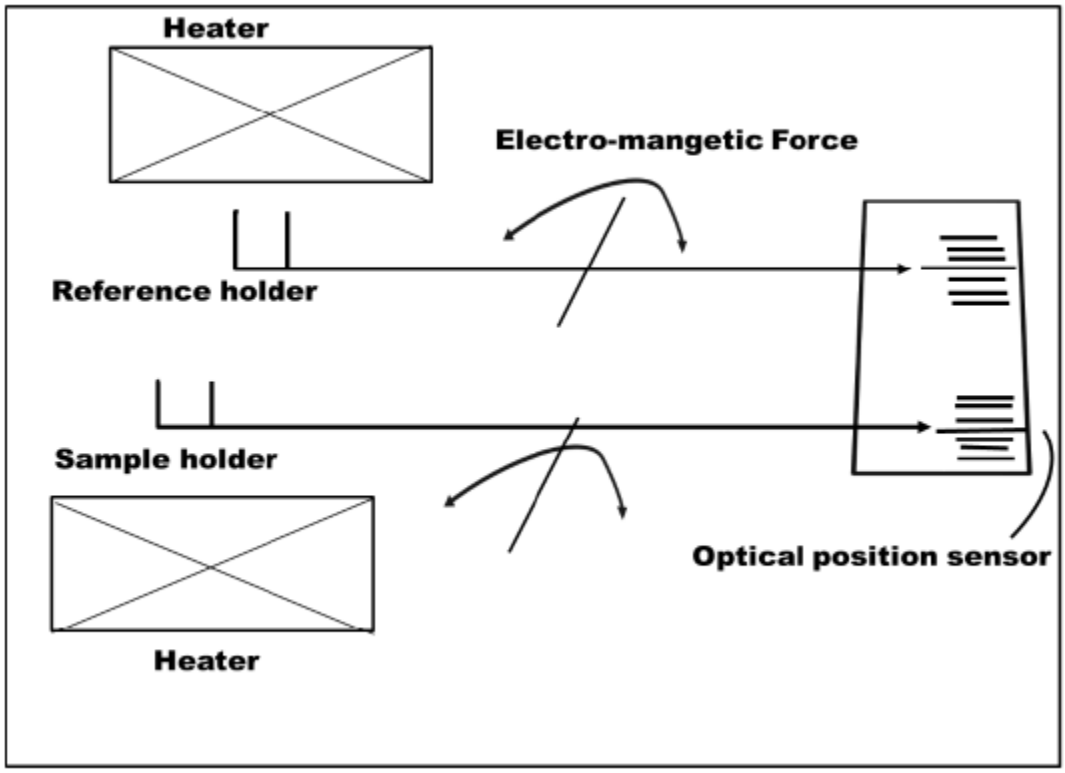

Fig 3.3: Schematic presentation STA measurement Principle of TGA (STA-7200)

The nitrogen is purged at a rate of 200 mL/minute into the balance bearing the sample, followed by a purge at a rate of 25 mL/minute. The equipment was calibrated according to the calibration protocol included with the instrument, using alumina and/or indium as calibration standards.

3.6 SURFACE AREA ANALYSIS

The Braunauer-Emmett-Teller (BET) method is a useful tool for determining the specific surface area of porous materials. A nitrogen purging system, vapors pressure measures, a temperature sensor and pressure transducer, as well as other connectors, are all standard equipment for this test. Surface area and volume of the pores in the porous MOF sample were evaluated applying the BET method by the application of the N_2 adsorption-desorption method using Micromeritics Instrument Corporation Tri StarIIPlus surface analyzer system. An adsorption isotherm, which is measured by the quantity of gas adsorbed at various pressures at a constant liquid nitrogen temperature (77K), is usually considered for BET analysis, followed by a desorption isotherm, which is measured by the amount of gas removed at lower pressure. The formula for calculating surface area is as follows:

$$\frac{1}{w\left[(P_0/P)-1\right]} = \frac{1}{W_m c} + \frac{C-1}{W_m c}\left(\frac{p}{p_0}\right)$$

Where w is the weight of the gas adsorbed, P_0 and P are the equilibrium and saturation pressure of adsorbates, v is adsorbed gas quantity, W_m is the adsorbate monolayer and c is the BET constant given by

$$c = \exp\left(\frac{E_1 - E_L}{RT}\right)$$

From the above equation, a linear plot of 1/ W (P/P0-1) vs. P/P0 gives rise to a slope of C-1/W_mC and intercept of 1/W_mC. The total surface area is the calculated by

$$S = \frac{W_m N A_{CS}}{M}$$

Where N is the Avogadro's number, M is the Molecular weight of the adsorbate and $A_{cs}$is theadsorbate cross sectional area.

The following procedure was used to examine the surface area of porous MOF materials under certain experimental circumstances. Before beginning N_2 adsorption, the MOF samples were degassed at 200°C under vacuum. To eliminate the N_2 gas, the sample was put at a high temperature under vacuum. The sample was held under high vacuum in the sample tube. It's submerged in a liquid nitrogen coolant bath. The amount of gas adsorbed was determined by measuring the sample pressure. The above-mentioned formulae were used to compute the surface area of the samples.

3.7 TRANSMISSION ELECTRON MICROSCOPY

The surface appearance and porosity of the compounds were studied using Transmission Electron Microscopy (TEM). In TEM, a high-energy electron beam contacts the crystal surface and travels in a variety of directions. The high kinetic energy is commonly produced by emitting tungsten filaments or lanthanum-based compounds, such as Lanthanum hexaboride. An external electric field ranging from 100 to 1000 kV accelerates the released electrons. The high-voltage electrons interact with the surface electrons of the samples, collecting material information. The transmitted electrons are analyzed for information such as the

specimen's size and shape. The transmitted intensity of electrons is measured as a function of angle, phase, and energy using a detector. High-resolution TEM pictures aid in the knowledge of surface microstructure and, in some cases, the analysis of materials at the atomic level.

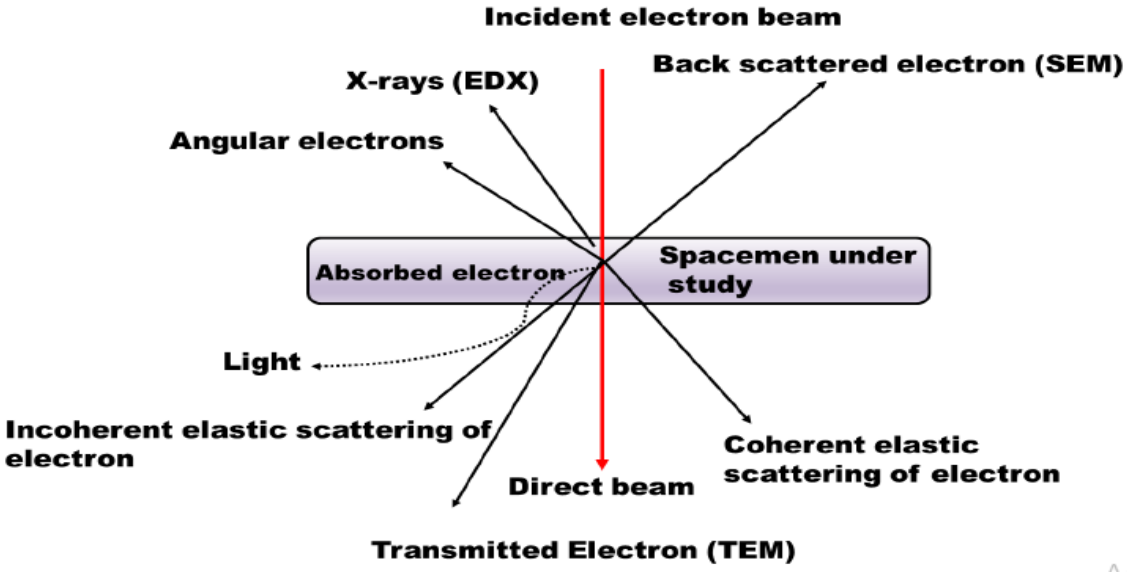

Fig 3.4: Schematic illustration of Transmission Electron Microscope

The powder samples of porous materials were dispersed in acetone/ethanol and then placed onto a support grid or films, as is standard method in sample preparation. A CCD camera was used to analyze the transmitted electrons after high-kinetic-energy electrons were steered onto the specimen. Certain precautions were taken when doing this experiment, which are listed below. The sample specimen was thinned to allow enough electrons to pass through for high-resolution photographs. Generally, these studies were carried out with kV Ultra High-Resolution TEM Microscope.

3.8 CYTOTOXICITY EXPERIMENT

MTT assays on raw 267.4 (1104cells/mL) were used to assess the cytotoxicity of MOFs and drug-loaded MOFs. Macrophages were cultivated in a 96-well plate containing DMEM media and incubated for 24 hours at 370°C with 5% CO_2 flow before being treated with various concentrations of manufactured MOFs and drug-loaded MOFs and incubated for another 24 hours. MTT solution was then added to the 0.1g/mL concentration well and incubated in the dark for 4 hours. MTT was reduced to formazan crystals, which were dissolved in medium (11 g sodium dodecyl sulphate in 50mL 0.02M HCl + 50mL isopropanol). The cell viability was assessed by comparing treated and untreated cells using an ELISA spectrophotometer (Biotek, Germany) at 570 nm [21, 22].

3.9 MOLECULAR DOCKING

Different characteristics of molecules are currently examined microscopically using a computer method. We used molecular docking to gain a better understanding of the interaction of MOFs, dye, and medicinal molecules. We investigated the molecular docking of MOFs with dyes and medicinal compounds to determine the binding locations. This docking computation was done with the Auto Dock Vina software. By eliminating the faulty contacts with the Auto Dock Tools (ADT) suit, Kollman charges and polar hydrogen were calculated. For this research, the Lamarckian Genetic Algorithm (LGA) was applied. Discovery studio visualizer 4.0 software was used to visualise all of the conformations, except for one that bonded well at the active site.

4. MAJOR APPLICATIONS OF MOFs

The unique properties of MOFs applicable in various field. We discuss here some of the major applications of MOFs.

4.1 GAS STORAGE AND SEPARATION

There are various methods for properly storing gas, but all of them demand a high-pressure tank and a multistage compressor. For practical purposes, these technologies are prohibitively expensive, and a simpler and less expensive alternative is required. Several materials, such as Zeolite or activated porous carbons, have been researched for gas storage to overcome these difficulties and discover safer storage solutions. MOFs offer a distinct advantage over other materials in this scenario. MOFs are preferred over other porous materials because of their simple preparation processes, high surface area, numerous functionalization options, and tunable pore structure.

More than 300 MOFs have been tested for H_2 storage. MOF-177, which consists of $[Zn_4O]$ clusters and 4, 4', 4"-benzene-1, 3, 5 – triyltribenzoate (BTB) to create (6, 3) net, is one of the most promising MOFs for this purpose. It has a gravimetric H_2 uptake of 7.5 wt% at 70 bar and 77 K due to its high surface area (5000 m^2g^{-1}) and large pore volume. MOF-5 (IRMOF-1), made of $[Zn (OAc)_2]$ and terepthalic acid, has a BET surface area of 3800 m^2g^{-1} and absorbs 7.1 weight percent at 40 bar and 77 K. Other H_2 storage materials include MOF-210, MIL-101, HKUST-1, NU-100, PCN-12, NOTT-102, and MOF-205. MOFs with open metal sites often have a large surface area, which allows for a greater interaction between the metal ion and the H_2 molecule. The high H_2 uptake in MOFs is primarily due to this factor. At 56 bar and 77 K, NU-100 has the maximum surplus H_2 storage capacity of 99.5 mgg^{-1}. At 80 bar and 77 K, MOF-210 has the largest overall H_2 storage capacity, with a value of 176 mgg^{-1}. Furthermore, it has been observed that doping MOFs with metal ions can improve H_2 uptake capacity. MOFs require less energy to release adsorbed hydrogen than other H_2 storage systems like transition metal hydrides. The hydrogen that has been produced can be utilized in the vehicle and fuel cell industries.

MOFs are said to be effective for lowering CO_2 levels in the atmosphere. MOF-210, for example, has the greatest surface area (10450m^2g^{-1}) of any MOF known to date, and is made up of 4,4',4"-[benzene-1,3,5-triyl-tris(ethyne-2,1-diyl)] tribenzoate (H_3BTE), biphenyl-4,4'- dicarboxylat (H_2BPDC), and zinc(II)nitratehexahydrate. CO_2 absorption is 2400 mg g-1 (74.2 wt%, 50 bar at 298K), which is higher than any other porous material. Under identical experimental conditions, MOF-200 and MOF-210 had equivalent CO_2 uptake. Other well-known MOFs with significant CO_2 absorption include NU-100 (69.8%, 40 bar at 298 K), Mg-MOF-74 (68.9%, 36 bar at 278 K), MOF-5 (58.9%, 10 bar at 273 K), and HKUST-1 (19.8%, 1 bar at 298 K). In comparison to unfunctionalized counterparts, the presence of polar groups such as —NH_2 or free N containing organic heterocyclic residues on the pores has also been proven experimentally and theoretically to help with high CO_2 uptake. BioMOF-11, for example, has shown the effects of an N-heterocycle, and its CO_2 consumption of 15.2% (at 1 bar and 298 K) is higher than any other MOF in the same category.

The first methane sorption investigation on MOFs was conducted by Noro *et al.* [23]. In a PCN-14 [Cu_2(adip), Adip = 5,5'-(9,10 anthracenediyl)di-isophthalate] MOF with a BET surface area of 1753 m^2g^{-1}, Zhou and colleagues demonstrated methane uptake of 16 wt% (35 bar). Other MOFs with high methane absorption capability include HKUST-1 (15.7 wt. %at 150 bar), MIL-101 (14.2 wt. % at 125 bar), IRMOF-1 [228 cm^3 (STP) g^{-1} at 298 K and 36 bar], and MOF-210 (264 mg g-1). The dominating factor responsible for the high methane capacity of Ni-MOF-74 [190 cm^3 (STP) g^{-1} (298 K, 35 bar) is open metal sites. Other significant hydrocarbons, such as benzene, toluene, xylene, and linear hydrocarbon, have been successfully isolated from liquid mixtures using MOFs.

MOFs can also be used to separate hazardous gases such as CO and NO from gas mixtures. Though CO separation in MOFs has not been achieved experimentally, the interaction between the CO dipole and open metal sites in MOFs is thought to be the most important component in sorption performance. MOFs, on the other hand, have been utilized to capture NO gas, such as Cu-SIP-3 and Zn (TCNQ-TCNQ) (bpy) [TCNQ = 7, 7, 8, 8-tetracyano-p-quino dimethane, bpy =4, 4'-bipyridyl]. These two

MOFs are normally nonporous and do not absorb gases such as Ar, N_2, CO_2, or CO_2, however they have been reported to absorb NO gas (9 molecules per formula unit at 1 bar) above the gate – opening pressure. The desorption path is not the same as adsorption when the pressure is reduced. Allen and colleagues reported the explanation for the aforementioned two MOFs' poor performance in 2010. In the case of Cu-SIP-3, strong coordination to coordinatively unsaturated metal sites (CUMs) is important, whereas charge transfer is important for high NO capture in [Zn (TCNQ-TCNQ)(bpy)]. At room temperature, Ni and Co-MOF-74 showed very strong NO absorption.

D. Yan et al. synthesised and studied the 1,2,4,5-tetrakis(3-carboxyphenyl)-benzene (m-H4TCPB) organic linker and its first metal-organic framework Cu-m-TCPB in 2014. At 77K and 1 atm, this molecule can absorb 24.4 cm^3g^{-1} $H^2$and 2.3 cm^3g^{-1} N^2. At 273 K and 1 atm, it has been reported to have absorption capacities of 23.3 cm^3g^{-1} acetylene, 23.0 cm^3g^{-1} CO_2, and 7.3 cm^3g^{-1}.

In addition to gaseous molecule absorption, several MOFs have also been developed that can adsorb water molecules. R. Banerjee and his colleagues established the capacity of chemically stable keto-enamine COFs to adsorb water in this direction.

4.2 MAGNETISM AND ITS APPLICATION

When paramagnetic 3d transition metal nodes are combined with suitable diamagnetic organic linkers, metal organic framework materials exhibit magnetism, and MOFs with magnetic properties are referred to as magnetic metal organic frameworks (MMOFs). The development of porous molecular magnets has been aided by first-row transition metal MOFs (V, Cr, Mn, Fe, Co, Ni, and Cu). Close-shell ligands [24] with weak magnetic interactions, such as cyano, oxo, azido bridges, and polycarboxylic ligands, are excellent candidates.

The framework structure of MOFs, which may comprise layered geometries with a shorter conjugated distance between metal clusters, is another cause for their magnetic behavior. MMOFs have also been synthesised using organic linkers, where the radicals in the organic linker are responsible for the magnetic characteristics. A number of MMOFs have been synthesised using this metal-radical combination approach.

A Ni-Glutarate based MOF[$Ni_{20}(H_2O)_8(C_5H_6O_4)_{20}.40H_2O$] exhibited ferromagnetic behaviour with a curie temperature of 4K due to weak ferromagnetic interactions of the Ni-O-Ni angle.At high temperatures, HKUST-1 is antiferromagnetic, whereas below 65K, it exhibits modest ferromagnetism. MIL-9, [$Co_5(OH)_2(C_4H_4O_4)_4$] has ferrimagnetic characteristics, according to reports. As multiferroics, Jain *et al* [26] reported four MOFs with the general formula [$(CH_3)_2NH_2$]M($HCOO)_3$ (M = Mn, Fe, Co, Ni).

Lanthanides form magnetic metal-organic frameworks instead of 3d transition metals. Two magnetic lanthanide-organic frameworks (LnOF) with the formulas [$Dy_2(bpa)_2(H_2O)_3$] and [$Er_4(bpa)_4(H_2O)_6$](H_2O) are made up of 1D rod-shaped metal carboxylate SBUs and 3,5-bis(4-carboxyphenoxy)benzoate (bpa3-) ligands. Magnetic MOFs can also be investigated for use in the elimination of arsenic in the environment. Magnetic nanoclusters have been found to be useful in the elimination of arsenic.

4.3 SENSING

Because aromatic units of linkers in most MOFs lead to excitation by absorbing UV-visible light and give luminescence, a large number of MOFs have been found to be photoluminescent. MOFs can be found in cathode ray tubes, fluorescent tubes, projection television, and X-ray detectors [26], small-molecule sensors, pH sensors [27], antennae in photo-sensitive bioinorganic compounds, photovoltaic light concentrators and high-tech optics as luminescent materials or phosphors.Because of their electronic transition from the d- to the f- shell, trivalent lanthanide metal ions are commonly employed in the synthesis of luminous MOFs. As luminous metal ions, lanthanides such as Eu, Tb, Dy, Sm, Nd, Gd, Er, and Yb

are employed. The most frequent ligands utilized to make luminous MOFs are naphthalene, anthracene, pyrene, perylene, and stilbene. Both the metal and the linker can produce luminescence, and they can also interact (via the antenna effect) to boost brightness and quantum yield. The use of bimodal (or multicoloured) emission in multiplexed detection and imaging of therapeutic cells is possible.Cation, anion, and molecule sensing are all applications for Ln-MOFs. One of the simplest and most powerful sensing mechanisms is a visible colour shift in material. For example, a nanotubular MOF, $\{[(WS_4Cu_4)I_2(dptz)_3].DMF\}_n$ (dptz =3,6-di-(pyridin- 4-yl)-1,2,4,5-tetrazine, DMF = N,N-dimethylformamide) was shown to be useful for detecting tiny solvent molecules. When different solvent molecules were accommodated as guests, the resulting inclusion compounds displayed diverse colours based on the solvent guests, demonstrating a new method of signal transduction as a new type of sensor. Water stable cationic MOF has recently been reported to be capable of adsorbing oxoanionic pollutants such as MnO_4- and $Cr_2O_7^{2-}$. For selective fluorescence quenching of an explosive TNP (2,4,6-trinitro phenol) in water an uratropin based MOFs are used as chemical sensor.

Another fascinating breakthrough is nano MOFs (NMOFs), which are used to detect pesticides. By developing an anti-paration/NMOF/2-ABA/ITO (ABA = 2-amino benzyl amine, ITO = Indium Tin oxide) sensing platform,the first biosensing application of Nano MOF $[Cd(atc)(H_2O)_2]n$ (atc = 2-amino terepthalic acid) impedimetrically for the detection of organo-phospat was demonstrated by Akash Deep *et al* [28].

Synthesizing photochromic MOF comprising 1, 4, 5, 8-naphthalenediimide (NDI) and Ca, Mg, Sr revealed their inkless printing property, demonstrating a novel strategy to developing an inkless and erasable printing medium employing MOFs. After 24 hours, the print content was self-erased. This could help to cut down on paper waste.

4.4 CATALYSIS

The presence of a strong metal–ligand interaction in MOFs can provide the material persistent porosity, allowing the solvent molecules to be removed completely without the structure collapsing. MOFs have demonstrated a lot of promise as a heterogeneous catalyst. MOFs with metal centres that are not totally blocked by organic ligands or with unsaturated, i.e. labile ligands are good catalysts because labile ligands are generally solvent molecules that leave a free coordination position on the metal when they are removed.The coordinated water molecule leaves a coordination vacancy on Cu when the $[Cu_3(btc)_2]$ (btc = 1,3,5-benzenetricarboxylate) material HKUST-1 is thermally activated.Nanoporous MOFs have been used to catalyse a variety of organic processes. For example, $[Cd(4\text{-}btapa)_2(NO_3)_2]$,(btapa = 1,3,5-benzene tricarboxylic acid tris[N-(4-pyridyl)amide]) or $[Cr_3F(H_2O)_2O(bdc)_3]$, (bdc = 1,4-benzenedicarboxylate) catalyse the Knoevenagel condensation reaction. Jing Xu et al. created a new bimetal complex $[Zn_4Ru_2(bpdc)_4.4C_2NH_8.9DMF]_n$ (H_2bpdc = 4,4'-biphenyldicarboxylic acid) that can adsorb Ru(II) photosensitizer $[Ru(bpy)_3]^{2+}$ and cobalamin derivatives like heptmethylcobyrinate perchlorate (B_{12}) to form a complex B_{12}-Ru@MOF. In the solid state, this compound has been shown to catalyse the dechlorination and 1, 2-migration reactions. This is the first time a MOF system has been used to catalyze B_{12} catalysis [29].

4.5 ELECTRAL PROPERTY AND ITS APPLICATION

MOFs have been shown to be an effective energy storage device material. Diaz *et al*. revealed the electrical storage capacity of MOFs in Co-doped MOF-5, i.e. Co_8-MOF-5[30] as electrode for supercapacitors. This MOF, on the other hand, has a substantially lower capacitance than commercially activated carbon. Lee et al. [31] presented a Cobalt-based MOF sheet exhibiting pseudocapacitorbehaviour, a specific capacitance of up to 206.76 F g^{-1} at 0.6 A g^{-1}, and an energy density of 7.18 Wh kg^{-1}. A flowerlike microsphere on a Zn-doped Ni-based MOF with a high specific capacitance (1620 Fg^{-1} and 860 F g^{-1} at 0.25 and 10 A g^{-1}, respectively), good rate capability, and strong cycle stability (91 percent for the MOF with Zn/Ni of 0.26). The electrochemical energy storage capability of 23 distinct nanocrystalline MOFs (nMOFs) was published in 2014. Among these nMOFs, nMOF-867, a zirconium-based MOF, has a high capacitance. The stack and areal capacitances of nMOF-867 are 0.64

and 5.09 mF cm^{-2}, respectively, which are nearly six times greater than those of activated carbon supercapacitors. A Mn-based MOF has recently been used as an active coating material to improve the capacity of Li-rich layered $Li(Li_{0.17}Ni_{0.20}Co_{0.05}Mn_{0.58})O_2$ oxide as a cathode for Li-ion batteries. This surface modified oxide material demonstrated a high discharge capacity, strong thermal stability without compromising cycle stability, high initial coulombic efficiency, and high rate capability. To further investigate the uses of MOFs, more research in this direction is required.

4.6 BIOMEDICAL APPLICATION

MOFs have a large drug loading capacity as well as a long release time. MOFs can load four times more medication than mesoporous silica materials, i.e. ibuprofen adsorption (up to 1.4 gm per gmof MOFs) with a longer release duration (up to 21 days). MOFs that are non-toxic can be used in targeted drug delivery. Because of their improved stability, massive porosity, and high pore volume, the MIL family of metal-organic frameworks is a viable candidate for storing and regulated release of biologically essential molecules.Serrey and Férey *et a*l [32] showed that encapsulating drug molecules (ibuprofen) in chromium carboxylate MOFs, MIL – 100 and MIL – 101, with drug storage capacities of 35 and 140 wt%, respectively, and regulated drug release behavior of 5 to 6 days under physiological circumstances. MIL-88A, MIL-8, MIL-100, and MIL-101 are iron(III) carboxylate MOFs that can entrap anticancer , antitumor, and antiviral medicines, as well as aesthetic agents.Férey *et al*·[32] presented the first group of synthesised MOFs for drug administration using trivalent metal centres with carboxylic acid bridging. A new type of magnetic MOF composite $Fe_3O_4/Cu_3(BTC)_2$, fabricated by combining Fe_3O_4 nanorods with $Cu_3(BTC)_2$nanocrystals (HKUST-1), adsorbed up to 0.2 gm of Nimesulide (an anticancer drug for pancreatic cancer treatment) per gramme of composite and took up to 11 days to release the entire drug in physiological saline at 37°C. By integrating camptothecin into ZIF-8 nanospheres, Zhuang *et al* proved ZIF-8 as a pH responsive drug delivery system with high cellular absorption efficiency. Cell death was increased when ZIF-8 was encapsulated [33]. Bernini et al. demonstrated the ability of GCMC (Grand canonical montecarlo) simulation to predict the microscopic performance of new porous MOFs in drug delivery applications and validated their simulation with available experimental data for ibuprofen adsorption-release in MIL-53(Fe), MIL-100(Fe), and MIL-101(Cr). Their calculation projected that mesoporous BioMOF-100 will have an exceptional ibuprofen adsorption capacity of 1969 mg g^{-1}, which is six times greater than the values published for mesoporous silica. Due to the presence of charge compensating ions in MOFs, strong electrostatic interactions improve the adsorbate-adsorbent interaction, resulting in greater drug loading at low pressure. The presence of dimethylammoniumcations in the pores of BioMOF-100 enhances the favourable interaction with ibuprofen molecules. The drug absorption capability of two distinct mesoporous MOFs, MIL-101 and UMCM-1, was also computationally compared using Monte Carlo simulation [34].

The antibacterial activity of the new MOF STAM-1 was compared to that of the HKUST-1 against the growth of Clostridium difficile, Staphylococcus aureus, and Pseudomonas aeruginosa. Both MOFs are discovered to have a strong inhibitory effect on the proliferation of these infections. When these MOFs are impregnated with NO, their antimicrobial activity is increased.

5. PROPERTIES AND FUNCTIONALIZATION OF MOFs FOR DRUG DELIVERY

In the introductory part we already discussed that the MOFs have various properties like ultrahigh porosity, tunable surface area, flexibility, charge conductivity, hydrophobicity and high thermal and chemical stability make it too special in various application. These properties are enabling the desired molecule to enter inside the framework and also make it stable inside. Therefore, of our drug delivery systems these properties are taking prominent rule. As traditionally many individuals organic and inorganic porous material are utilize for drug delivery. But these materials have not such porosity and stability. These materials are frequently releasing their inside molecule and also some poor biocompatibility issue make it unfavorable for DDS. Here in this field MOFs eliminate all such problem in large extent.so MOFs are used widely in DDS. In addition of these inherent

properties functionalization of MOFs are required for the better drug delivery. In this section we discuss the important functionalization strategy which required for biomedical application and especially in the field of drug delivery. Such functionalization's are pore encapsulation, surface adsorption, covalent binding, and functional molecules as the building block, which is discussed one by one.

5.1 SURFACE ADSORPTON

Functional molecules can be adsorbed on the surface of MOFs due to their large surface area and porosity. The pre-synthesized MOFs are stirred in a solution of functional molecules to achieve surface adsorption. The primary forces in this approach are Van der Waals interaction, π–π interaction, and hydrogen bonding. There are no strict requirements for the pore size or type of functional groups of MOFs when using this relatively simple strategy. However, due to the weak interaction forces between molecules and the MOF framework, the leaching problem is difficult to avoid.

Surface adsorption has been widely used to immobilize enzymes. The Balkus group reported in 2006 that physical adsorption of microperoxidase-11 (MP-11) catalyst on a nano-crystalline Cu-based MOF while maintaining MP-11 catalytic activity [35]. MP-11 based on Cu- MOF outperformed five mesoporous benzene silica (MBS) host materials in terms of catalytic activity. Liu et al. created enzyme–MOF bioreactors for catalysis using MOFs that had not been chemically modified on the surface. Hydrogen bonding and π–π interaction are primarily responsible for facilitating host–guest interactions, according to studies [36, 37]. Ma et al. [38] created an integrated electrochemical biosensor by co-immobilizing methylene green (MG) and glucose dehydrogenase (GDH) in zeoliticimidazolate frameworks (ZIFs). ZIF-70 had the best adsorption capacity for MG and GDH out of a set of ZIFs with varying pore sizes, surface areas, and functional groups.

Nucleic acids, in addition to enzymes, can be immobilized on MOFs via surface adsorption. The Zhou and Deng group, for example, created four isoreticular MOFs (Ni- IRMOF-74-II to -V) with tuned open channel sizes ranging from 2.2 to 4.2 nm to precisely include single-stranded DNA (ssDNA) [39]. By confining the nucleic acid chain completely inside the channel, the MOF framework acted as an excellent host to protect ssDNA from degradation. According to research, van der Waals interactions in Ni-IRMOF-74-II are responsible for the reversible uptake and release of ssDNA, which is enabled by a suitable channel size and moderate accommodation. The Ni-IRMOF-74 series was then used as non-viral vectors for intracellular delivery and gene silencing.

5.2 PORE ENCAPSULAION

Many different types of functional molecules can be accommodated inside the pores of MOFs due to their high porosity and pores that can be tunable from microporous to mesoporous. MOFs serve as a host material, preventing leaching and protecting the loaded substrates from external factors. Pore encapsulation via de novo synthesis is a versatile and efficient method for incorporating functional molecules into MOFs. MOF formation and substrate encapsulation occur simultaneously during the synthetic process. As a result, this method allows for the immobilization of larger molecules into the cavity of MOFs that are larger than the pore size of MOFs. The substrate must, however, be stable under synthetic conditions.

This method has been widely used in the past to encapsulate anticancer drugs inside the MOF host for intracellular delivery and subsequent release. Monodisperse ZIF-8 nanospheres of uniform article size (70 nm), for example, were synthesized with the anticancer drug camptothecin encapsulated within the framework. Studies on the MCF-7 breast cancer cell line revealed improved cell internalization and decreased cytotoxicity. The anticancer drug 3-methyladenine was successfully incorporated into ZIF-8 by combining inorganic metal salts, organic ligands, and drug molecules. In HeLa cells treated with 3-methyladenine@ ZIF-8 nanoparticles, autophagy inhibition was found to be more effective. Because of its good monodispersity, optimal size for cellular

uptake, ease of synthesis under mild conditions, and ease of surface modification, ZIF-8 has been considered an ideal host material for intracellular drug delivery.

Enzyme encapsulation by de novo synthesis has been accomplished in addition to anticancer drugs. Wu et al. described a simple one-step synthesis of ZIF-8 nanocrystals containing glucose oxidase (GOx) and horseradish peroxidase (HRP) in aqueous solution at 25 °C [40]. The GOx&HRP@ZIF-8 bioconjugates demonstrated excellent stability, selectivity, and catalytic efficiency. Hou et al. encapsulated GOx in magnetic ZIF-8 to create a reusable multi-enzyme mimic system [41].

In general, the synthetic conditions of MOFs, such as high temperature, organic solvents, and an acidic environment, are too harsh for biomolecules like enzymes to maintain their structural features and activities. Pore encapsulation using a post-synthetic modification technique provides a potent route for integrating biomolecules under mild circumstances, which was used to overcome this issue. The Ma group reported immobilization of microperoxidase-11 (MP-11) into a mesoporous MOF, dubbed Tb-mesoMOF, in 2011 [42]. The enzyme with dimensions of about 3.3 × 1.7 × 1.1 nm^3 was successfully loaded into MOFs with cages of 3.9 and 4.7 nm in diameter by immersing freshly synthesized Tb-mesoMOF crystals in MP-11 solution. MP-11@Tb-mesoMOF demonstrated higher catalytic activity than mesoporous silica material (MCM-41). Later, the researchers discovered that cytochrome c (Cyt c) with dimensions of 2.6× 3.2 ×3.3 nm^3 could be captured by a MOF with smaller window sizes (1.3 and 1.7 nm) [43]. According to mechanistic studies, the enzyme was adaptable and could significantly change its conformation in order to pass through small nonporous and enter the MOF's interior. Similarly, the Zhou group created a stable PCN- 333 with large mesoporous cages that served as single-molecule traps (SMTs) for enzyme encapsulation, preventing enzyme aggregation and leaching [44]. PCN-333(Al) was effectively encapsulated with three distinct enzymes, with record-high loading and recyclability.

5.3 COVALENT BINDING

Despite the fact that surface adsorption and pore encapsulation methods have been used to include diverse functional molecules into MOFs, the comparatively weak contact forces between these molecules and MOFs frequently result in delayed leaching difficulties. Immobilization by covalent binding appears to be a viable option in this case.

The MOF surface has a variety of functional groups, including amino, carboxyl, and hydroxyl groups, which can be used to establish covalent connections with reactive groups on the target [45]. Jung et al., for example, used post-synthetic alterations to conjugate enhanced green fluorescent protein (eGFP) and Candida antarctica lipase B (CAL-B) enzymes on the MOF surface [46]. To activate the dangling carboxylate groups of organic ligands on the MOF surface for subsequent bio conjugation, a coupling reagent such as 1-ethyl-3-(3-dimethylaminopropyl) carbodiimide (EDC) or dicyclohexylcarbodiimide (DCC) was used. Enantioselectivity and activity in the trans-esterification of (±)-1-phenylethanol were found to be well conserved for CAL-B-MOF bioconjugates in studies. The protease enzyme trypsin has been successfully immobilized on MIL-88B (Cr), MIL-88B NH_2 (Cr), and MIL-101(Cr) using a similar coupling approach [47]. This was accomplished through the nucleophilic attack of trypsin's amine groups on DCC-activated MOFs. The effectiveness of BSA protein digestion by Trypsin-MIL-88B-NH_2 (Cr) was comparable to that of native trypsin digestion. In addition to the carboxylate group, the amino group on organic ligands can be used to link with enzymes such glucose oxidase and soybean epoxide hydrolase.

Biomolecules have been immobilized using the click reaction on organic linkers. The first nucleic acid–MOF nanoparticle conjugates were reported by the Mirkin group [48]. A strain-promoted click reaction involving azide-functionalized UiO-66 and dibenzylcyclooctyne-functionalized DNA was used to make them. The DNA strands were coordinated to the exterior surface of MOF nanoparticles due to the tiny pore size of UiO-66. During the chemical reaction, the UiO-66 structure might be preserved. The DNA–MOF conjugates outperformed nonfunctionalized MOF nanoparticles in terms of colloidal stability and cellular absorption.

Inorganic metal clusters, in addition to organic linkers, provide another form of reactive site in MOFs for covalently binding functional molecules. The Mirkin group reported a generic and straightforward strategy to using oligonucleotides to functionalize the exterior surface of MOF nanoparticles in 2017 [49]. The exterior metal nodes of MOF nanoparticles were covalently coupled with terminal phosphate-modified oligonucleotides using a coordination chemistry-based method. On the exterior surface of nine different archetypical MOFs containing different metals (Zr, Cr, Fe, and Al), oligonucleotides were successfully changed. This approach enables for particle surface functionalization regardless of MOF structure. Furthermore, DNA can be chemically manipulated to modify interparticle interactions. The nucleic acid nanoparticle conjugates generated could be employed for DNA-mediated programmable assembly and regulation of intracellular processes. Using the accessible coordination sites on Zr_6 clusters, the Zhou group described a simple one-pot method for incorporating a succession of porphyrin derivatives into stable Zr-MOFs [50]. Tunable concentrations of tetratopictetrakis(4-carboxyphenyl) porphyrin (TCPP) ligands were successfully integrated by combining ligands of varied geometries and connectivities while maintaining the crystal structure, morphology, and ultrahigh chemical stability of the parent MOF. This method made it simple to make multifunctional stable Zr-MOFs for future uses.

5.4 FUNCTIONAL MOLECULE AS BUILDING BLOCK

Designing functional molecules as the building block is another way to functionalize MOFs. Inorganic metals can coordinate with various reactive chemical groups found in biomolecules. As organic ligands, amino acids, peptides, nucleobases, and saccharides have been used to construct bio-MOFs thus far. Bio-MOFs have a higher level of biocompatibility and biological functionality. However, because most biomolecules are very flexible and have little symmetry, using them directly to make high-quality MOF crystals is difficult.

Several oxygen and nitrogen atoms in the structure can be used as lone pair electron donors to coordinate with metal ions in nucleobases. Because of the extensive binding modes given by four N atoms in the purine ring and one exocyclic amino group, adenine has been widely investigated to develop bio-MOFs [51]. A symmetrical co-ligand was used to drive the synthesis of a highly ordered MOF structure using low-symmetry adenine as the building block. The Rosi group created crystalline and porous bio-MOF-1 with the formula $Zn_8(ad)_4(BPDC)_6O.2Me_2NH_2.8DMF.11H_2O$[52] by mixing biphenyldicarboxylic acid (BPDC), adenine, and zinc acetate dihydrate. The MOF is made up of infinite 1D zinc-adeninate columns that are joined by linear BPDC linkers and comprise corner-fused zinc-adeninate octahedral building units (ZABUs). The same group later reported bio-MOF $100(Zn_8(ad)_4(BPDC)_6O_2.4Me_2NH_2.49DMF.31H_2O)$, a mesoporous MOF with a larger surface area (4300 $m^2\ g^{-1}$) and pore volume (4.3 $cm^3\ g^{-1}$). The MOF is made up of distinct ZABUs linked together by BPDC linkers. To create a three-dimensional structure with enormous holes and channels, each ZABU is connected to four surrounding ZABUs by 12 BPDC linkers.

6. DRUG LOADING AND CHARACTERIZATIONS

6.1 METHOD FOR DRUG LOADING

MOFs are recognized by their highly organized structure and enormous surface area. Drugs can be enclosed in inter pores or imbedded on the outer surface using a variety of loading methods. The one-step method and the two-step method, which are both extensively used loading procedures, are summarized below.(Fig 6.1)

6.1.1 ONE STEP

The most convenient loading strategy for incorporating pharmaceuticals into MOFs is the one-step method, which can be accomplished either during MOF synthesis or by directly employing drug molecules as MOF linkers.

6.1.1.1 CO-CRYSTALLIZATION

It is frequently utilized in laboratory research and manufacturing for medication loading. Drug could co-crystallize with MOFs under mild reaction conditions, forming a 3D supramolecular structure that integrates the active compounds. More importantly, co-crystallization has no effect on the drug's physicochemical properties, which can be used to improve loading efficiency and solubility. Poorly soluble medicines like IBU, lansoprazole, leflunomide, and methotrexate (MTX), for example, were successfully embedded in -CD-MOFs using the co-crystallization approach, with drug loading equal to or higher than that achieved by impregnation.

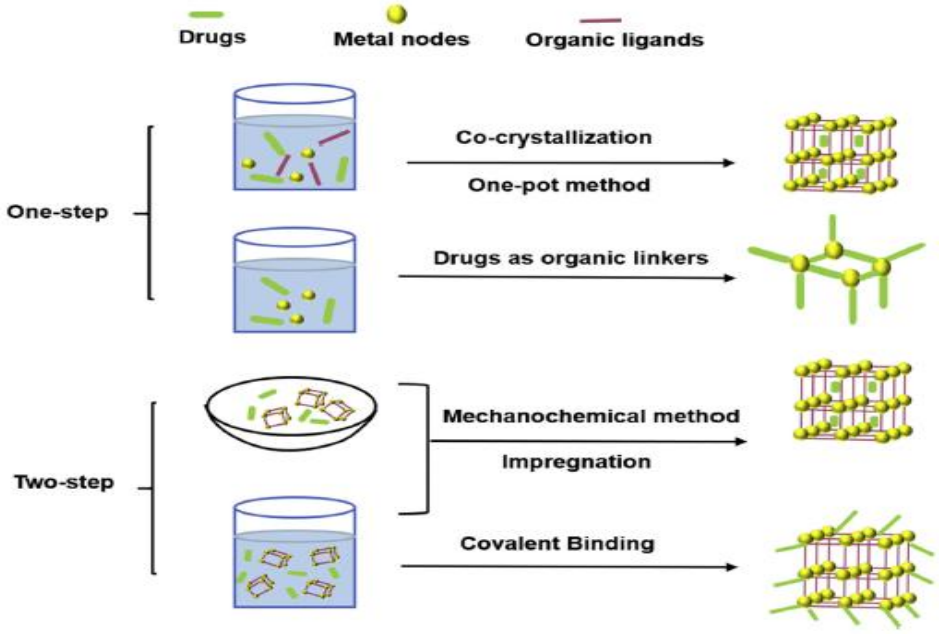

Fig 6.1 -Two kinds of drug-loading strategies for MOFs.

6.1.1.2 ONE POT METHOD

It is a cost-effective approach for loading drugs into MOFs during synthesis that not only saves reaction time and waste, but also overcomes the limits of MOFs' tiny pore window. Drug molecules could be loaded in MOFs matrix using this method by putting them inside MOFs crystals or coating them on the surface. Furthermore, certain MOFs have pore diameters that are too small for medicines to permeate the crystalline matrix. Because the pore cavity of ZIF-8 is 11.6 Å in diameter, many bulky compounds such as high-molecular-weight medicines, nucleic acid, and proteins cannot permeate into the porosity of MOFs. Nonetheless, effective encapsulations of pharmaceuticals such as DOX, camptothecin, and 3-methyladenine have been obtained by mixing reactants in a one-pot technique. Similarly, utilising a one-pot manufacturing process, 5-FU could be loaded on zinc glutamate MOF coated cotton fabric. Furthermore, enzymes embedded in MOFs by this approach were not degraded. Organic linkers and inorganic metal ions both contributed to the successful inclusion of the enzyme in the one-pot approach as an in situ loading strategy. MOFs were formed as a result of the protein molecules, which aided in their crystallisation. Using the one-pot method, Cytochrome c (Cyt c) was directly immobilised in ZIF-8.Cyt c@ZIF-8 has a 10-fold higher peroxidase activity than free enzyme. Similarly, Wu *et al.* [53] used the similar strategy to design a ZIF-8-based multi-enzymatic system. To make GOx&HRP@ZIF-8, the zinc nitrate solution was combined with glucose oxidase (GOx) and horseradish peroxidase (HRP). Catalytic testing revealed that the GOx&HRP@ZIF-8 composite was more efficient than either GOx@ZIF-8 or HRP@ZIF-8.

6.1.1.3 DRUG AS ORGANIC LINKERS FOR MOFs

Drugs or their prodrugs can be used as organic linkers to construct MOFs, in addition to MOFs as reservoirs, by coordinating the available coordinated functionalities of drugs with certain metal nodes. A phosphonate MOF-based DDS with variable release rate pattern [54] was constructed using medically acceptable ions Ca (II) and Mg (II) as metal ions and anti-osteoporosis bisphosphonate model pharmaceuticals (e.g., etidronate, pamidronate, alendronate, and neridronate) as organic linkers.

6.1.2 TWO STEPS

The two-step technique involves either immersing medications with MOFs in a drug solution or grinding MOFs with drugs.

6.1.2.1 IMPREGNATION

Drug molecules diffused into MOFs through the porosity after the MOFs were immersed in drug solution. Van der Waals interaction, π-π- interaction, and hydrogen bonding are the most common interactions between medicines and MOFs. MOFs' pore size, window dimension, chemical composition, and flexibility were all important factors in ensuring drug incorporation. MOFs were used to load caffeine by impregnation. To implant the medication into the 2D channels, Javanbakht *et al*. [55] submerged porous Cu-MOFs in an IBU solution. The CD-MOFs cavities may be impregnated with the poor-soluble medication honokiol using a supercritical carbon dioxide ($scCO_2$) assisted impregnation approach with a high drug loading of 40.78 % (w/w). Furthermore, due to the close interaction between phosphate groups and Fe ions, this technique achieved about 100% efficiency in the case of phosphate drugs. With a satisfactory drug loading capacity of 30% (w/w) and outstanding encapsulation efficacy rates of >98%, gemcitabine monophosphate (GEM) was encapsulated into MIL-100(Fe).

6.1.2.2 MECHANOCHEMICAL METHOD

It is a solvent-free, environmentally friendly, and cost-effective drug loading process that involves mechanically mixing drug powder and MOFs in a solid state. By grinding drugs such as 5-FU, caffeine, p-aminobenzoic acid, and benzocaine into MOFs, high drug loading amounts and prolonged release were achieved.

6.1.2.3 COVALENT BINDING

Despite the fact that the appeal technique inserts diverse pharmaceuticals into MOFs, the comparatively weak contact force between cargos and MOFs frequently results in gradual drug leaching problems. As a result, a covalent bonding and immobilization solution is required. MOFs have numerous active groups (e.g., carboxyl, amino, and hydroxyl) on their surfaces that can be utilized to form covalent bonds with reactive groups of active drugs. Morris *et al.* [56] showed that a click reaction between azide-functionalized UiO-66 and dibenzylcyclooctyne-functionalized DNA produced a DNA-MOF compound. In comparison to nonfunctionalized UiO-66, the DNA@UiO-66 conjugate was found to have better colloidal stability and cellular transfection capabilities. Covalent binding can also be used to successfully immobilize enzymes on MOFs. Cao *et al.* [57] used a cross-linking technique to successfully immobilize soybean epoxide hydrolase onto the prepared surface of UiO-66-NH_2 MOF. The produced soybean epoxide hydrolase@UiO-66-NH_2 conjugates had a higher loading capacity, better enzyme-substrate binding affinity, and higher catalytic efficiency than free soybean epoxide hydrolase.

6.2 CHARACTERIZATION OF DRUG LOADED MOFs

The pore size and surface property of MOFs are important parameters that are strongly related to drug loading efficiency (Eq. 1) and encapsulation efficiency (Eq. 2).

$$\text{Loading efficiency } (\%) = \frac{\text{Mass of loaded drug}}{\text{Mass of drug loaded MOFs}} \times 100 \quad (1)$$

$$\text{Encapsulation efficiency } (\%) = \frac{\text{Mass of loaded drug}}{\text{Mass of total drug}} \times 100 \quad (2)$$

When the loaded drug is greater than the pore diameter of the MOFs, the drug can be physically adsorbed on the surface of the MOFs using the impregnation approach. In most cases, using the one-step technique may efficiently encapsulate large sized pharmaceuticals inside MOFs, resulting in improved drug loading and encapsulation efficiency. Furthermore, by increasing drug-MOF interactions (hydrogen bonding or van der Walls), modifying the structure of MOFs may promote a higher drug loading level. The most common procedures for determining drug loading and encapsulation efficiency are dissolving drug-laden MOFs in a solvent to assess drug content and calculating loaded drug content by measuring the content of unloaded drugs supernatant. Furthermore, because a mass loss step occurs within a particular temperature range, TGA can be used to indirectly determine the concentration of adsorbed medicines in MOFs. Apart from this several instrumentation techniques are employed to determine the structure and properties of drug loaded or non-loaded MOFs, which is already discussed in the previous section 3(General characterization technique for MOFs).

7. CLASSIFICATIONS OF MOF FOR DRUG DELIVERY

MOFs are made up of a variety of linkers and metals that govern its polytrophic structure and properties (Fig. 7.1). Furthermore, fragile coordination bonds connect the linker with the metal cluster, improving biodegradability. However, in biological mediums, a delicate balance between degradability and adequate stability must be maintained. Specific applications, such as stimuli-responsiveness in drug delivery, pH responsive, molecular-responsive, thermo-responsive, and pressure-responsive MOFs, can be achieved by correctly selecting both the metal ion and the organic linker. MOFs studied primarily for DDSs are categorized in this review based on the presence of specific components and properties in their composition.

7.1 CLASSIFICATION BY METAL IONS

Because the number of ligands and metal ions is almost limitless, thousands of MOFs have been synthesised using a variety of metal ions and organic linkers. When MOFs are utilized in DDSs, they must be thoroughly pre-tested for biocompatibility and toxicity, which are directly related to their compositions [58]. Metals and linkers should both be nontoxic.

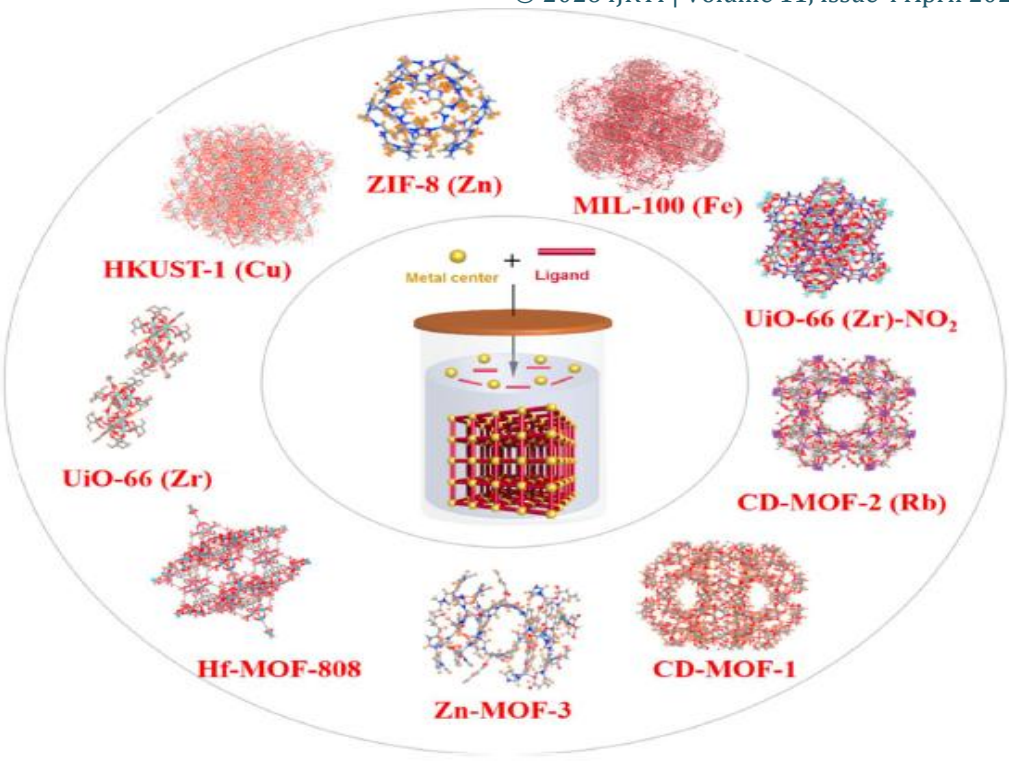

Fig 7.1 Representative MOFs crystal structures.

To estimate the toxicity of metals, the median lethal dosage (LD_{50}) is commonly used [59]. Furthermore, potassium, zinc, zirconium, and iron are recommended metals for DDSs with MOFs, with oral $LD_{50}$of 0.215, 0.35, 4.1, and 0.45 g/kg, respectively [60, 61]. Iron [62,63], zirconium[64,65], potassium[66,67] and zinc-based [68,69] MOFs are still the most commonly used for DDSs[70], with a variety of anticancer[71-73], antibiotics[74], and antiviral drugs[75,76] loaded into their porosities. Drugs can be co-loaded in MOF cages, providing synergies in the battle against diseases [74, 77]. In the pharmaceutical area, several other examples of MOFs as drug carriers have been documented, allowing for high drug payloads, higher drug solubility, improved stability, targeting abilities, and better bioavailability. As indicated in Table 1 [78, 62, 65, 71, 77-95] the MOFs for DDSs that have been described so far are classified according to their metal ions composition.

Table 1 Classification of MOFs by metal ions and their molecular pore size for drug loading.

Genre	Naming	Organic linker	Pore size (A°)	Drug loading	Ref.
Fe-MOFs	MIL-89 (Fe)	Muconic acid	11	Ibuprofen, azidothymidine triphosphate	71
	MIL-88A (Fe)	Fumaric acid	6	Ibuprofen, cidofovir	71
	MIL-100 (Fe)	1,3,5-Benzenetricarboxylic acid	25, 29	Gemcitabine-monophosphate, topotecan, isoniazid, doxycycline, tetracycline, docetaxel, azidothymidine triphosphate, lamivudine triphosphate	71,77,84,86–88
	MIL-101_NH_2 (Fe)	Amino 1,4-benzenedicarboxylic acid	29, 34	Azidothymidine triphosphate, cidofovir, ethoxysuccinato-cisplatin,Ibuprofen, oridonin	71,89
	MIL-53 (Fe)	1,4-Benzenedicarboxylic acid	8.6	Ibuprofen, azidothymidine triphosphate Caffeine	62,79
	MIL-101 (Fe)	2-Amino 1,4-benzenedicarboxylic acid 3,3′,5,5′-Azobenzenetetracarboxylate	25-30		71
	MIL-127		4		90
Zn-MOFs	Zn (TATAT)2/3 .3DMF.H_2O	TATAT = 5,5′,5″-(1,3,5-Triazine-2,4,6-triyl)Tris (azanediyl)triisophthalate	17, 21	5-Fluorouracil	91
	ZnBDP_X	1,4-Bis(1H-pyrazol-4-yl)-2-X-benzene (H2BDP_X; X Z H, NO2, NH2, OH)	11	Mitoxantrone	80
	Bio-MOFs	Azobenzene-4,4′-dicarboxylic acid and biphenyl-4,4′-dicarboxylic acid	8.3-26	Etilefrine hydrochloride	92
	$Zn_8(O)_2(CDDB)_6$	4,4′-(9-H-Carbazole-3,6-diyl) dibenzoic acid	28.1 x	5-Fluorouracil	81

	$(DMF)_4(H_2O)$ ZIF-8	2-Methylimidazolate	23.17 11.6	5-Fluorouracil, doxorubicin	 93,94
Zr-MOFs	UiO-66 UiO NMOFs UiO-66-NH_2/NO_2	1,4-Benzenedicarboxylic acid Amino-triphenyldicarboxylic acid 1,4-Benzenedicarboxylic acid	8 - -	Caffeine, dichloroacetate Cisplatin prodrug, siRNAs Ketoprofen	65,90 95 82
K-MOFs	CD-MOF-1	Cyclodextrins	4-17	Lansoprazole, azilsartan, budesonide, valsartan	78,83,84,96
Cu-MOFs	HKUST-1 MOF-2/MOF-3	1,3,5-Benzenetricarboxylic acid 1,3,5-Benzenetricarboxylic acid and isophthalic acid	14.67 21.2/20.9	Ibuprofen Ibuprofen, doxorubicin hydrochloride	85 85

7.1.1 Cr-MOFs

In 2006, two model systems, chromium-based MOFs (Cr-MOFs), designated MIL-100 (Cr) and MIL-101 (Cr) (MIL stands for Materials of Institut Lavoisier), which are made up of trimers of metal octahedra and di- or tricarboxylic acids, were used to evaluate drug loading into MOFs. MIL-100 (Cr) had Cr (III) ions and 1, 3, 5-benzenetricarboxylic acid (BTC) or trimesic acid, whereas MIL-101(Cr) contained terephthalic acid and Cr (III) [97, 98]. Ibuprofen (IBU), a typical model drug, was loaded in Cr-MOFs, demonstrating strong drug loading capability of up to 1.4 g IBU per grams of dehydrated MIL-101 (Cr), although MIL-100 (Cr) absorbed only 0.35 g IBU.

7.1.2 Fe-MOFs

The above-mentioned MOFs are not suitable for biomedical applications because to Cr toxicity. Soon after, MIL-53 (Fe) iron-based MOFs (Fe-MOFs) based on Fe (III) octahedra and terephthalate anions were synthesized [79]. They emerged as potential candidates for drug delivery spontaneously due to their low toxicity, structural flexibility, and biodegradability. The first nanosized Fe-MOFs [71] were successfully used for loading anticancer or retroviral medicines, and their degradability, biosafety, and imaging characteristics were demonstrated in *vitro* and in *vivo*.Leng et al. [62] chose the nontoxic and biocompatible MIL-53 (Fe) to load anti-cancer medication oridonin, and the drug loading capacity could reach 56.25 percent (w/w) with a sustained release period of more than 7 days, owing to the flexibility of Fe-MOFs. Furthermore, Fe-MOFs were investigated for drug loading and magnetic/fluorescence imaging at the same time [63].pH-controlled drug release was observed in hollow Fe-MOFs-5-NH_2 with a drug loading capacity of up to 35% (w/w). The MOFs developed have excellent magnetic resonance imaging (MRI) performance due to the presence of Fe (III) ions. Targeted drug distribution and fluorescence imaging were achieved following

modification using folic acid (FA) and fluorescent reagent. MIL-100 (Fe) was also utilised to co-encapsulate two potent triphosphorylated nucleoside reverse transcriptase inhibitors, azidothymidine triphosphate and lamivudine triphosphate, to improve anti-human immunodeficiency virus (HIV) [77] efficacy. MIL-100 (Fe) had the same azidothymidine triphosphate/lamivudine triphosphate ratio as currently available triple therapy based on HIV prodrugs, with a total drug loading of 9.6% (w/w). After freezedrying, drug-carrying particles could be stored for up to two months while maintaining identical physicochemical features.

7.1.3 Zn-MOFs

Zinc-based MOFs (Zn-MOFs) was developed by Rojas *et al.* [80] in 2016 as four zinc pyrazolate isoreticular MOFs ZnBDP_X composed of Zn (II) and functionalized organic linkers 1,4- bis(1H-pyrazol-4-yl)-2-X-benzene (H_2BDP_X; X Z H, NO_2,NH_2, OH) for intravenous and oral administrations (<200 nm). This ZnBDP X family had square channels with a free pore aperture of 11 A° and a tetragonal form. In *vitro* tests in relevant biological circumstances revealed favorable structural and adhesive durability. Then, two types of anticancer medicines, mitoxantrone and Ru (p-cymene) Cl_2 (1,3,5-triaza-7-phospaadamantane) (RAPTA-c), were encapsulated within the pores of the ZnBDP X to see how the differing functional structures affected drug packing and delivery. Bag et al. [81] created a stable bicarboxylate ligand 4, 40-(9-H carbazole-3, 6-diyl) dibenzoic acid (H_2CDDB) for creating Zn-MOFs in order to improve the water stability and therapeutic activity of MOFs. A porous MOF $[Zn_8(O)_2(CDDB)_6$ $(DMF)_4(H_2O)$ was created by reacting Zn $(NO_3)_2.6H_2O$ and H_2CDDB in dimethylformamide (DMF) with an excellent loading ability of 53.3 % (w/w) for 5-fluorouracil (5-FU). Furthermore, this MOF can stay stable in water for three weeks, and a 12-hour MTT experiment against human hepatoblastoma cell line (HepG2) and human breast ductal carcinoma cell line (MDA-MB-435S) revealed that it is biosafe.

ClO_4^- anion as template and 5-(40-carboxyphenoxy) nicotinic acid (H_2cpon) as organic linker [99] was used to create another Zn-MOF, Zn-cpon-1, with a 3D topological framework. This Zn-cpon-1 with pH-responsive twofold stimulation activity was an excellent drug delivery vessel, with a loading capacity of 44.75 % (w/w) of 5-FU in Zn-cpon-1. The drug release behaviour, in particular, was consistent with the Weibull distribution model, which was dual-irrigated by pH and heating. In DDSs [100-102], zeoliticimidazolate frameworks (ZIFs), a sub-family of Zn-MOFs, are commonly employed. ZIFs are coupled by Zn(II) and imidazolate or its derivatives. Sun et al. [102] used ZIF-8 to use a one-pot technique to pack the volatile and hydrophobic D-a-tocopherol succinate, with a drug loading ratio of 43.03 % (w/w). Due to the pH-responsiveness of ZIF-8, the obtained D-a-tocopherol succinate@ZIF-8 would rapidly breakdown in an acidic environment, resulting in on-demand drug release for tumour chemotherapy.

7.1.4 Zr-MOFs

Since Cavka*et al.* [124] discovered Zr_6 $(m_3\text{-}O)_4$ $(m_3\text{-}OH)_4(BDC)_6$ (UiO-66, UiO stands for the University of Oslo) with $Zr_6(m_3\text{-}O)_4$ $(m_3\text{-}OH)_4(CO_2)_{12}$ clusters and 1,4-benzene-dicarboxylate (BDC) in 2008, zirconium-based MOFs (Zr-MOFs), primarily Zr(IV) carboxylates, have received increasing attentions. They have unmatched stability, notably hydrothermal stability [64], because to the high oxidation state of Zr(IV) in Zr-MOFs and the strong coordination interactions between Zr(IV) and carboxylate ligands in the vast majority of carboxylate-based Zr-MOFs. As a result, many Zr-MOFs are stable in organic solvents and water, even in acidic environments. Furthermore, due to its widespread distribution in nature and low toxicity in vivo (oral fatal dosage LD50w4.1 g/kg) [103], Zr is regarded acceptable for biomedicine.

In the field of biomedicine, Zr-MOFs are commonly employed. Aba'nades *et al.* [65] discovered that delivering dichloroacetate and 5-FU from Zr-MOFs to cancer cells in a synergistic manner can improve cytotoxicity *in vitro*. By accelerating pit-mediated endocytosis and cytoplasmic drug distribution, changing particle size and, more crucially, surface chemistry can increase cytotoxicity. Li et al. [82] also developed UiO-66 with $-NH_2$ and $-NO_2$ functional groups to investigate the differences in

drug loading capacity and release behavior. Because of the strong hydrogen bond ability and alkaline features of -NH_2, the findings revealed that UiO-66NH_2 had the highest loading of ketoprofen and the lowest release rate.

Zr-fum, a kind of Zr-MOF with an endogenous fumarate linker and a structure similar to UiO-66, is another type of Zr-MOF. Zr-fum is stable in aqueous solutions and has a lot of potential as a DDS. During the manufacturing process, the anticancer chemical dichloroacetate was incorporated into Zr-fum as a size-controlled modulator, with payloads of 20% (w/w) [104]. In contrast to UiO-66, Zr-fum showed improved biocompatibility due to the endogenous fumarate linker and more efficiently delivered the drug imitator calcein into HeLa cells.

7.1.5 K-MOFs

Smaldone et al. [105] originally reported cyclodextrin-based metalorganic frameworks, a renewable, highly symmetric and porous, ultrahigh surface area edible MOF made entirely of edible ingredients: potassium (K) ions, alcohol (ethanol), and cyclodextrin (CD-MOFs). CD-MOFs have a wide range of applications in the biomedical field [67] owing to their porous properties aside from their water-soluble and non-toxic nature. As a result, this hotspot is garnering a lot of attention and evolving at a quick pace. Drugs have been successfully loaded onto CD-MOFs [106] via impregnation, grinding, and co-crystallization thus far. For example, lansoprazole embedded CD-MOFs were synthesised utilising an improved co-crystallization process including gamma -CD and K(I) ions, with a drug loading of up to 23.2 % (w/w)[83]. Furthermore, CD-MOFs can improve the bioavailability and solubility of insoluble medicines significantly. He et al. [78] found that loading azilsartan (AZL) into CD-MOFs boosted AZL bioavailability by 9.7 times in Sprague-Dawley (SD) rats. Furthermore, as compared to pure medicines, AZL/CDMOF had a 340-fold increase in apparent solubility. Furthermore, CD-MOFs have been reported to be utilized in oral, intravenous, and even pulmonary DDSs [84, 107].

7.1.6 Cu-MOFs

Due to the great accessibility of their coordinatively unsaturated metal sites in the structures, which create strong binding sites for guest cargos [108-110], copper-based MOFs (Cu-MOFs) have been investigated as potential hosts for bio-oriented guest@MOF composite systems. Sun *et al*. [86] developed Cu-MOFs, MOF-2, and MOF-3 mixed ligands for the delivery of IBU and doxorubicin hydrochloride (DOX) using a hydrothermal technique with an acceptable change in the ratio of the two ligands (BTC and isophthalic acid). They were harmless to human normal cells and could load drug in human embryonic kidney 293A cells (HEK 293A). Drug loading tests revealed that mixed ligand MOFs had higher DDS capacity than single ligand MOFs, with MOF-2 containing 40% BTC and 60% isophthalic acid having the greatest drug delivery potential.Hou*et al*. [111] developed a smartphone-based strategy for visual detection of alkaline phosphatase that possessed oxidase mimic and fluorescence virtue, based on the characteristics of aminofunctionalized Cu-MOFs. This fluorescent-based technology might be used to detect alkaline phosphatase in serum samples, opening up the possibility of diagnosing other biomarkers in clinical serum samples using an enzyme-linked immunosorbent test mediated by alkaline phosphatase. Cu-MOFs could also be used as an antibacterial agent. Cu-MOFs containing glutaric acid and pyridine derivatives, for example, showed excellent antibacterial activity against a variety of microorganisms at very low minimal bactericidal concentrations [112].

7.2 CLASSIFICATION BASED ON ORGANIC LIGAND

The MOFs' versatility in terms of constitutive metals and organic linkers is one of its key advantages. Organic linkers, in particular, play an important role in the 3D supramolecularorganisation and physicochemical properties of MOFs. The most prevalent organic linkers are carboxylates and other organic anions such as phosphonate, sulfonate, and heterocyclic compounds. In fact, it has been stated that the range of probable linkers is exceedingly broad [113,114]. MOFs with carboxylate ligands account

for roughly half of all materials produced. In the case of MOFs for DDSs, the linker used has a significant impact not only on the physical and chemical properties of the resultant MOFs, but also on their biological stability, bioavailability, and toxicity.

The choice of linker produces unique features and MOF applications. Polycarboxylic acid or imidazole-based linkers, for example, are commonly used in the creation of MOFs due to their low toxicity, owing to their high polarity and metabolic clearance in physiological conditions [70]. Biosafe synthesis of homologous iron carboxylates is possible [115]. Different organic linkers and functional groups also alter drug payloads and release patterns in MOFs [70, 71,116].

Active molecules were utilized as linkers to create so-called BioMOFs, which is an interesting twist. This technique not only provides for high drug payloads due to active molecule intrinsic self-assembly, but it also allows for good biocompatibility. As building blocks, a variety of biomolecules such as amino acids, nucleobases, and sugars that are readily or naturally available can be used [117].Gramaccioli *et al*. [118], as far as we know, created the first amino acid-based biocompatible 3D MOFs in 1966 by combining Zn(II) with glutamate, a key neurotransmitter. However, the biomedical applications of BioMOFs have yet to be completely explored, owing to a dearth of studies on the stability of these systems in biological media. There are just a few instances of BioMOFs that can bind and release drugs [119]. There have been numerous publications on the utilisation of active components to make BioMOF, which is understandable given that many medicinal compounds have multiple complicated groups in their structures. The first drug-based BioMOF study was published in 2010, [120], and it was made up of endogenous iron and therapeutically active vitamin B3, with anti-pellagra, vasodilation, and anti-lipid characteristics. Similarly, olsalazine, a commonly used agent in the treatment of ulcerative colitis and other gastrointestinal disorders, could be used as a ligand for the fabrication of a series of new mesoporous MOFs, and had the same coordinating functionality as the dihydroxyterephthalic acid used in the CPO-27/ MOF-74 family composite.Here, MOFs are catalogued according to their Bio-organic linkers, as shown in Table 2 [71, 83, 85, 90-93, 98,120,122].

Table 2 Classification of MOFs by organic linkers.

Family of linkers	**Organic linker**	**Drug loading**	**Ref.**
Carboxylate ligands	1,3,5-Benzenetricarboxylate acid	Doxorubicin	85
	4,4′,4″-Benzene-1,3,5-triyl-tribenzoate	Ibuprofen	98
	5,5′,5″-(1,3,5-Triazine-2,4,6-triyl) tris(azanediyl)triisophthalate	5-Fluorouracil	61
	Biphenyl-4,4′-dicarboxylic acid	Hydrochloride	92
	Azobenzene-4,4′-dicarboxylic acid	Etilefrine	92
Pyrazolate ligands	Bis (pyrazolate) ligand (1,4-bis(1H-pyrazol-4-yl)-2-X-benzene (H_2BDP_X; X = H, NO_2, NH_2, OH)	Mitoxantrone	90
Imidazolate	2-Methylimidazolate	5-Fluorouracil	93
Polysaccharide	Cyclodextrin	Lansoprazole	83
	Other polysaccharides (agar, dextran)	Procainamide	

BioMOFs	Nicotinic acid	Vitamin B_3	120
	Succinic acid	Cisplatin	122
	Fumarate ligands	Doxorubicin	71

8. APPLICATIONS OF MOFs IN THERAPY AND DRUG DELIVERY

8.1. MOF SYSTEMS FOR DISEASE THERAPIES

MOFs have been investigated as potential DDSs for a variety of diseases, including infections, lung disease, diabetic mellitus, ophthalmic disease, and malignancies, due to their superior drug delivery properties.

8.1.1. ANTI-BACTERIAL APPLICATION

In view of bacteria resistance and bacterial infection in the injury and surgical process, smart distribution of antibacterial agents is of great importance.Although inorganic [125] and organic polymer [126]carriers have been proposed for targeting antibacterial DDSs, their instability, poor biocompatibility, and uncontrolled release characteristics limit their antibacterial uses. MOFs with a hybrid organic-inorganic structure have recently been investigated for antibacterial therapy. Lin et al. [127] investigated MOF-53(Fe) containing iron ions and BDC as a carrier for antibacterial drugs due to its chemical stability in an acidic environment.Vancomycin, a glycopeptide macromolecule antibiotic, was physically integrated into MOF-53(Fe) NPs. The medication loading of vancomycin could be as high as 20% (w/w). Furthermore, under bacterial infection conditions, MOF-53(Fe) displayed a slower and more regulated drug release profile with 99.3% antibacterial efficacy against *Staphylococcus aureus* (pH = 5.5). MOF-53 (Fe)@vancomycin, on the other hand, showed outstanding biocompatibility and chemical stability *in vitro*.

Intracellular bacterial infections are particularly difficult to treat because germs can lurk inside cell components, evading immune system surveillance.Gallis et al. [128] loaded ceftazidime, a third-generation broadspectrum cephalosporin, using ZIF-8. High resolution STEM-EDS elemental mapping was used to confirm the successful loading of ceftazidime in ZIF-8. During the first day of the drug release test in PBS, % of the ceftazidime was released at pH 5.0, whereas 50 percent was released at pH 7.0. Gramnegative *E. coli* was used to test the antibacterial abilities of pristine ZIF-8 and ceftazidime@ZIF-8 particles. After 24 hours, there was no difference between them, but ceftazidime@ZIF-8 showed nearly complete growth inhibition of E. coli at 50 mg/mL, whereas pristine ZIF-8 showed no antibacterial effect after 72 hours, implying that the antibacterial effectiveness was dependent on the degradation of ceftazidime@ZIF-8. Furthermore, confocal imaging was used to directly observe particle internalization in cells, proving that this technology may be used for intracellular bacterial killing. Zhang *et al* [129] reported yet another ZIF-8 antibacterial use. Tetracycline was encapsulated in MOF in a single step during the synthesis of ZIF-8. Tetracycline was encapsulated in MOF in a single step during the production of ZIF-8. Furthermore, tetracycline@ZIF-8 was coated with hyaluronic acid (HA) via coordination enabling active-targeting of bacteria within the cell. This tetracycline@ZIF-8@HA nanocomposite (TZH) has the potential to release antibiotics in a pH-responsive manner. More importantly, Zn (II) and antibacterials produced by ZIF-8 may work together to combat germs. TZH could also remove intracellular bacteria more effectively with the help of HA, resulting in a significant reduction in antibiotic usage. Finally, TZH had a clearance rate of above 98 percent for intracellular microorganisms.

MOFs have primarily been studied in the antibacterial sector as drug carriers, with only a few researches examining how MOF diameter, shape, and surface modification effect cellular internalization. MIL-88 (A) and MIL-100 (Fe) particles, both combined with mannose for active targeting and constructed with rod-like and spherical morphologies respectively, are

investigated by Guo et al. [130] as a possible bacteria-mimicking delivery approach for intramacrophagic-based infections. MIL-88 (Fe) had a rod shape with a long-axis size of 3628-573 nm and an aspect ratio of 1:5, whereas MIL-100 (Fe) had a spherical shape with a diameter of 103.9- 7.2 nm and an aspect ratio of 1:5. MIL-100 (Fe) NPs were internalized faster in a cell internalization test, but mannosylation had no effect on MIL-100 (Fe) uptake because the rate and extent of uptake were sufficient, whereas cellular uptake of MIL-88A (Fe) was greatly increased. Furthermore, the predominant internalisation mechanism in MOF particle uptake was shown to be micropinocytosis/phagocytosis.

In orthopaedics, infection prevention and osseointegration promotion are two major goals. Yu et al. [131] created naringin-loaded MOF NPs that may be used to coat mineralized collagen. The release kinetics of naringin could be controlled with MOF NPs to improve osseointegration and prevent bacterial infection. The coating performed exceptionally well for mesenchymal stem cells in terms of adhesion, proliferation, osteogenic differentiation, and mineralization, according to the findings. Meanwhile, the antibacterial efficiency against *S. aureus* was improved, indicating that this orthopaedic coating might be used on implants. Because of the release of Ag (I) ions and the formation of reactive oxygen species (ROS) [132], ultrafine silver (Ag) NPs have been found to be a promising antibacterial agent in numerous studies. Ultrafine Ag NPs, on the other hand, are usually unstable and quickly aggregated [133]. By exploiting the mesoporosity of gama-CD-MOFs in one pot, Shakya et al. [134] reported a template-assisted synthesis of ultrafine Ag NPs with a size of roughly 2 nm, achieving Ag NP stability improvement. In addition, the Ag@CD-MOFswere cross-linked and surface modified with the GRGDS peptide to increase wound hemostasis. The anti-bacteria and hemostasis tests revealed that the GS5-CL-Ag@CD-MOFs were an excellent technique for combining hemostasis and antibiosis.

Due to the restricted antibacterial efficiency of single-model bactericidal methods, high-dose use and sluggish sterilisation rates are common, and it is critical to design a dual bactericidal system. Yang et al. [135] created a MOF/Ag-derived nanocomposite with superior metal-ion-releasing ability and forceful photothermal conversion capability for synergistic sterilization, consisting of metallic Zn and a cgraphitic-like carbon framework. Massive heat was created when bacterial membranes were subjected to near-infrared irradiation, while bacterial internal components were destroyed by abundant released Zn(II) and Ag(I) ions from MOF-derived nanocarbon. Furthermore, in systematic antibacterial testing, the nanocomposite showed less cytotoxicity while having an excellent antibacterial activity.

8.1.2. LUNG DISEASE THERAPY

For lung diseases such as asthma, respiratory tract infections, chronic obstructive pulmonary disease, and lung cancer, pulmonary medication delivery can produce very efficient tailored therapeutic therapy. MOFs can be employed as carriers for pulmonary medication administration because of their customizable structure, porosity, and inhalable size. Hu *et al.* [84] recently used g-CD-MOF to load budesonide for dry power inhalers that had been modified with cholesterol (CHO) and leucinepoloxamer. The particle size distribution revealed that more than 90% of the particles were within the acceptable diameter range of 1-5 mm for inhalation. Furthermore, in vitro, treatment with CHO improved the flowability and aerodynamic properties of CD-MOF. Most notably, in vivo animal tests revealed that a dry power inhaler based on CHO-CD-MOF could be a promising pulmonary delivery carrier.

Mohamed *et al.* [136] used MIL-89 and PEGylated MIL-89 (MIL-89 PEG) as carriers for pulmonary arterial hypertension delivery in another study. Both had particulate sizes between 50 and 150 nm, with the bulk of them being 100 -38 nm. MIL-89 PEG exhibited better form homogeneity and stability after PEGylation. MIL-89 and MIL-89 PEG were found to be harmless to endothelial cells in cell tests. Furthermore, both of them inhibited inflammation in macrophages. In addition, in vivo studies demonstrated that MIL-89 was well-tolerated for a short period of time and accumulated in the lungs, suggesting that it could be a good carrier for pulmonary arterial hypertension medications.

To obtain better control and tailored therapy, tuberculosis treatment requires a mix of drug delivery and imaging. Pulmonary administration of anti-tuberculosis drugs is an ideal technique for maintaining local therapeutically effective concentrations while avoiding significant systemic exposure and side effects. Wyszogrodzka et al. [137,138] utilized Fe-MIL-101-NH_2 NPs as carriers for regulating the release of isoniazid (INH) and an MRI contrast agent. Fe-MIL-101-NH_2 was found to be safe in *in vitro* cytotoxicity tests, and cell internalization investigations supported its use in tuberculosis treatment. Hydrophobic poly (lactide-co-glycolide) (PLGA) microparticles were used to load INH-MOF via spraydrying, then mixed with spray-dried INH-MOF-loaded D-leucine (LC) microparticles to improve the aerodynamic properties of INH-loaded MOF (INH-MOF). Finally, the INH-MOF-loaded PLGA/LC demonstrated outstanding aerodynamic characteristics, regulated INH release, and good macrophage internalisation. The Fe ions in INH-MOF could also be used as an MRI contrast agent to monitor particles after inhalation.

Due to their pH sensitivity and reversible aggregation properties, discovered that Fe(III) polycarboxylate based nanoMOFs were capable of targeting lung tissue. After intravenous delivery, the nanoMOFs generated microaggregates that were retained in the lung capillaries due to the neutral pH of the blood. The agglomerates disaggregated and began to decompose after 24 hours, resulting in drug release with enhanced therapeutic impact compared to free drug and a reduction in metastasis. The proper timing of reversible aggregation/disaggregation was particularly consistent with tissue function, reducing toxicity concerns.

8.1.3. DIABETES THERAPY

Diabetes mellitus is still a major health issue all over the world. To maintain euglycemia, type 1 diabetes requires continuous insulin injections. The importance of developing an effective and improved insulin delivery system cannot be overstated. For achieving glucose responsiveness, the most studied insulin delivery systems are based on GOx, which is frequently supplemented with pH responsive materials.Duan*et al*. [138] looked into a simple one-pot method for making an enhanced glucose-responsive insulin delivery system, in which insulin-GOx/ZIF-8 was self-assembled from a mixture of Zn(II), 2-methylimidazole, GOx, and insulin. When blood glucose levels were greater than normal, GOx accelerated the conversion of glucose to gluconic acid, which prompted ZIF-8 to disintegrate and release insulin. Furthermore, when glycemic levels reached normoglycemic levels, ZIF-8 insulin secretion dropped, preventing hypoglycemia.

Yang et al. [140] recently developed a unique approach for transdermal insulin administration by integrating multi-enzyme Co-ZIF-8 containing insulin and GOx as repertories with microneedles. Co(I) ions in ZIF-8 MOFs were created to act as a biomimetic catalase, decomposing excess H_2O_2 and preventing injury to normal tissue. Meanwhile, free Co(I) ions can be chelated in microneedles using ethylene diaminetetraacetic acid modified SiO_2 NPs, then peeled away. The generated MOF-based microneedles demonstrated good insulin release capability depending on glucose concentration without H_2O_2 and Co leakage, according to the results (I).

Diabetic foot ulcers are a severe concern for diabetics, and there are currently no viable treatments available. FA modified Cu-MOFs (F-HKUST-1) were created by Xiao *et al*. [110] for the treatment of chronic nonhealing wounds. FA was added to the HKUST-1 formula to decrease the release of Cu (II) ions, which resulted in faster wound healing and less toxicity. In vivo studies demonstrated that F-HKUST-1 can enhance angiogenesis, collagen deposition, and re-epithelialization, as well as speed up wound healing.

8.1.4. OCULAR DISEASE THERAPY

Ophthalmic medications that are prepared as eye drops are typically cleared quickly from the eyes, reducing their ocular bioavailability to less than 5%.As a result, Kim *et al*. [141] used NH_2-MIL-88 (Fe) for continuous brimonidine release in order to

improve its ocular bioavailability. Brimonidine was absorbed into the vast internal pores of NH_2-MIL-88 by physical absorption (Fe). Furthermore, the amino groups and hydrogen-rich organic ligands in this MOF established hydrogen bonds with the hydroxyl groups and inherent carboxyl of mucin chains, resulting in mucoadhesive characteristics and increased drug retention in the preocular.*In vitro* tests in NH2eMIL-88 revealed that the encapsulated medication was released in a continuous manner (Fe). Furthermore, in the *in vivo* test, the bioavailability of brimonidine was increased in NH_2-MIL-88 (Fe) when compared to the marketed product (Alphagan-P). Despite the fact that this MOF can be completely decomposed into Fe (III) and 2-amino BDC in physiological fluid in half a day, the long-term presence of Fe (III) may pose a risk to ocular safety.

Gandara-Loe*et al* [142] conducted another study using Zr-based UiO-67 loaded brimonidine tartrate and polyurethane nanocomposite films as new ocular treatments. Due to the massive tetrahedral and octahedral cages of UiO-67, this functional MOFs-based ocular polymeric device displayed good adsorption and release performance for brimonidine tartrate and achieved a regulated and extended drug release in glaucoma therapy.

8.1.5. ANTI-TUMOR APPLICATION

For the treatment of malignancies, developing innovative DDSs to improve chemotherapy effectiveness and reduce adverse responses makes a lot of sense. MOFs have been used to improve drug accumulation in tumours as nanocarriers with high drug loadings and facile customization. Zhang *et al.* [143] used ZIF-8 to co-deliver chemotherapeutic medicines DOX and P-glycoprotein (P-gp) inhibitor verapamil hydrochloride (VER) to multidrug-resistant tumour cells, resulting in enhanced drug concentrations. DOX and VER were co-incorporated into ZIF-8 using a one-pot strategy, and then (DOX+ VER)@ZIF-8 was functionalized with poly (ethylene glycol)-folate (PEG-FA) by coordination to achieve longer circulations and active targeting, resulting in increased therapeutic efficiencies and significantly safer properties than free DOX.

Cancer starvation therapy based on GOx has been touted as a possible treatment option. However, the low efficacy of GOx administration and self-limiting curative impact have limited its use. Zhang *et al.* [144] used ZIF-8 as carriers to encapsulate GOx and the prodrugtirapazamine, which they subsequently packed with an erythrocyte membrane to create a biomimetic nanoreactor tirapazamine-GOx-ZIF-8@erythrocyte membrane. ZIF-8's vast cavities would allow for a high loading efficacy of GOx, shielding it from leaching, aggregation, and catalytic activity loss. The erythrocyte membrane may aid in evading immunity and prolonging blood circulation, allowing GOx to be delivered to tumour cells for the exhaustion of intracellular glucose and oxygen. The resultant tumour hypoxia triggered the activation of tirapazamine, allowing for more effective colon cancer treatment. Jiang *et al.* [145], for example, employed ZIF-8 to codeliverquercetin as an anticancer medication and CuS NPs as a photothermal therapy (PTT) agent for improved synergistic tumour treatment. The use of ZIF-8 to integrate quercetin, a promising anticancer drug with poor water solubility and chemical instability, could considerably reduce quercetin's drawbacks. PTT has gotten a lot of attention because of its low invasiveness and high selectivity. Huang *et al.* [146] investigated *in situ* production of MIL-53 (Fe) nanocomposites, taking advantage of pyrrole monomer oxidation in the cage to create polypyrrole NPs. MIL-53's wide surface area, porosities, and original structure remained constant after polymerization, allowing it to load DOX for chemotherapy. Meanwhile, the Fe ions in MIL-53 would operate as a T2 MRI contrast agent, allowing researchers to trace the composites' dispersion. The produced PPy@MIL-53/DOX with excellent drug loading capability and photothermal action demonstrated good therapeutic synergism, according to the results.

Photodynamic therapy (PDT) with the potential to generate cytotoxic singlet oxygen via photosensitizers (PS) is also a promising technique for the treatment of malignant tumours, in addition to chemotherapy and PTT. However, PDT treatment-induced oxygen consumption might result in irreversible tumour spread and medication resistance. As a result, creating new O_2-generating materials to give O_2 to the tumour microenvironment would considerably improve PDT's effectiveness against hypoxic tumours. The pore diameters, high characteristic surface area, and porous structure of tunable MOFs give them good gas

storage capacity. Gao*et al.* [147] used UiO-66 as a depot for O_2 storage, then conjugated with indocyanine green (ICG) to create a biomimetic O_2-evolving PDT nanoplatform (O_2@UiO-66@ICG@RBC). Finally, the membranes of red blood cells (RBCs) were coated to facilitate immune escape. When exposed to laser irradiation at 808 nm, $^1O_2$ produced by ICG damaged the RBC membrane and promoted O_2 release from UiO-66, improving PDT effects. To maintain redox homeostasis, the concentration of GSH, an important intracellular antioxidant, was reduced in response to the intracellular damage caused by $^1O_2$. It's worth noting that GSH consumption was linked to ferroptosis, which is a Fe-dependent cell death that's distinct from other types of cell death. Meng et al. [148] used a disulfide-containing imidazole as an organic ligand and Zn(II) as matching coordination metal ions to develop a MOF-based nanocarrier for combining PDT with ferroptosis, and then encapsulated a photosensitizer chlorin e6. Upon light irradiation, GSH depletion caused by \schlorin e6-loaded MOF through the disulfide-thiol interaction resulted in the inactivation of glutathione peroxide 4 which was linked to ferroptosis, thus, achieving an augmentation of anticancer PDT by the MOF nanocarrier.

Min *et al.* [149] reported another study combining PDT with anti-angiogenesis therapy, using porphyrinic MOF nanostructure as antiangiogenic drug delivery carrier and PDT agent, which was decorated with MnO_2 layer to neutralise excessive GSH in tumour for enhanced PDT therapy, then endowed with mouse breast cancer cells (4T1) membrane to achieve tumortargeting ability. Following intravenous delivery, the multi-functionalized porphyrin Zr-MOF would selectively concentrate in tumours via homologous targeting mediated by tumour cell membrane camouflage, followed by improved PDT via GSH consumption and release of the antiangiogenic medication apatinib. Furthermore, because of its MRI contrast quality, Mn(II) produced from MnO_2 could be employed for in vivo tumour imaging.

Haddad et al. [150] recently created a mitochondria targeting DDS for cancer therapy based on MOF, employing UiO-66 as carriers to carry anti-cancer medication dichloroacetate, then conjugating with triphenylphosphonium for mitochondria targeting. Human breast cancer cell lines MCF-7 cells treated with the derived MOF showed mitochondrial morphological alteration followed by autophagy and cell death, according to super-resolution microscopy investigations. Furthermore, full transcriptomeanalysis revealed that when cells were treated with the targeted MOF, cellular gene expression was significantly altered, demonstrating that directing MOFs to mitochondria is a worthwhile method.

Carbon monoxide (CO) is recognised to be damaging to individuals because it has a higher affinity for haemoglobin than oxygen, which can be utilised to treat malignant tumours in conjunction with chemotherapy and PTT. Because of its toxicity, intracellular transport and on-demand release of CO are essential. Yao *et al.* [151] proposed a unique technique using Mn carbonyl modified PEGylated Fe(III)-based nanoMOFs (MIL- 100) enwrapped magnetic carbon NPs (MCM@PEG-CO) to realise near infrared spectroscopy light-responded CO gas therapy and chemotherapy combination. $Mn(CO)_5Br$ was used as the CO source in this method, and MIL-100 nano MOFs allowed for high DOX drug loading capacity. Meanwhile, MIL-100 modified with 4, 4-diamino-2,2-bipyridine (DABPY) would effectively immobilise$Mn(CO)_5Br$ for CO release control. Furthermore, the addition of a magnetic carbon core not only enabled PTT therapy by near-infrared spectroscopic irradiation, but also improved T_2 MRI, giving MCM@PEG-CO tumourdualmode imaging capabilities, including photoacoustic imaging and MRI.

More recently, a study revealed the first use of MIL-100 radioenhancers in combination with GEM , a radio sensitizing anticancer medication. Due to the activation of gama radiation, the MIL-100 regular porous framework with oxocentered Fe trimers detached by roughly 5 A° (trimesate linkers) was able to scatter the electrons emitted from nano-MOFs. As a result, cancer cells were harmed by water radiolysis and the formation of hydroxyl radicals. MIL-100 also carried their GEM into cancer cells. Both MIL-100 and GEM contributed to the synergistic enhancement of the radiation effect by demonstrating separate modes of action [152]. This research offered up new possibilities for the project of engineered NPs, in which each constituent played a role in radiotherapy-assisted tumour therapy.

9. CONCLUSIONS AND PERSPECTIVES

MOFs have been intensively explored for a range of applications over the last few decades due to their well-defined structure, high surface area, high porosity, variable pore size, and ease of functionalization. In recent years, there has been a lot of interest in using MOFs as nanocarriers for drug delivery in biological applications. Anticancer medicines, nucleic acids, and proteins are among the substances now being studied as therapeutic agents for disease treatment. We summarized four popular techniques for functionalizing MOFs with therapeutic agents for drug delivery in this review. Surface adsorption, pore encapsulation, covalent binding, and functional molecules as building blocks are only a few of them. The key forces involved in surface adsorption and pore encapsulation approaches include the van der Waals interaction, the π–π interaction, and hydrogen bonding. The covalent binding approach binds functional molecules to the framework using inorganic metal clusters or organic linkers. Furthermore, organic ligands can be used to introduce functional molecules into the framework. Then we went over the latest developments in biological applications of MOF nanocarriers for drug delivery. Many medicinal compounds have been successfully delivered using MOF nanoparticles, owing to the particular properties of MOFs.

Despite significant progress in this subject, there are still a number of difficulties to overcome. First, despite the fact that various functionalization strategies have been documented, they all have some drawbacks. Due to weak contact forces, molecules absorbed by surface adsorption and pore encapsulation, for example, leak gradually. Stronger connections are provided via covalent binding, although it necessitates sophisticated synthetic techniques and may affect the activity of useful molecules. Organic ligands suited for MOF synthesis, on the other hand, are typically rigid and extremely symmetrical, making it difficult to use biomolecules directly as a building block. Due to these constraints, enhanced functionalization procedures are needed to include a wide range of possible therapeutic compounds into MOFs and investigate their clinical uses. Second, the pharmacokinetics, in vivo toxicity, degradation mechanism, and drug loading and release kinetics of MOF nanoparticles are still being investigated. More research is needed to develop MOF–drug conjugates with improved bio-stability, biocompatibility, and therapeutic effectiveness. Finally, MOFs have unique features that make them promising candidates for intracellular drug delivery in the treatment of illnesses. To fully exploit the promise of MOFs as drug delivery systems in clinical applications, efforts should be concentrated on addressing the stated hurdles in the future.

10. REFERENCES

1. Hoskins, B. F.; Robson, R. Infinite Polymeric Frameworks Consisting of Three Dimensionally Linked Rod-like Segments. *J. Am. Chem. Soc.* **1989**, *111*, 5962–5964. https://doi.org/10.1021/ja00197a079.
2. Wang, Y.; Yan, J.; Wen, N.; Xiong, H.; Cai, S.; He, Q.; Hu, Y.; Peng, D.; Liu, Z.; Liu, Y. Metal-Organic Frameworks for Stimuli-Responsive Drug Delivery. *Biomaterials* **2020**, *230*, 119619. https://doi.org/10.1016/j.biomaterials.2019.119619.
3. Mueller, U.; Schubert, M.; Teich, F.; Puetter, H.; Schierle-Arndt, K.; Pastré, J. Metal–Organic Frameworks—Prospective Industrial Applications. *J. Mater. Chem.* **2006**, *16* , 626–636. https://doi.org/10.1039/b511962f.
4. Son, W.-J.; Kim, J.; Kim, J.; Ahn, W.-S. Sonochemical Synthesis of MOF-5. *Chem. Commun.***2008**, *47*, 6336. https://doi.org/10.1039/b814740j.
5. Forgan, R. S.; Smaldone, R. A.; Gassensmith, J. J.; Furukawa, H.; Cordes, D. B.; Li, Q.; Wilmer, C. E.; Botros, Y. Y.; Snurr, R. Q.; Slawin, A. M. Z.; Stoddart, J. F. Nanoporous Carbohydrate Metal–Organic Frameworks. *J. Am. Chem.* Soc.**2011**, *134*, 406–417. https://doi.org/10.1021/ja208224f.
6. Sha, J.; Yang, X.; Sun, L.; Zhang, X.; Li, S.; Li, J.; Sheng, N. Unprecedented α-Cyclodextrin Metal-Organic Frameworks with Chirality: Structure and Drug Adsorptions. *Polyhedron* **2017**, *127*, 396–402. https://doi.org/10.1016/j.poly.2016.10.012.

7. Ding, H.; Wu, L.; Guo, T.; Zhang, Z.; Garba, B. M.; Gao, G.; He, S.; Zhang, W.; Chen, Y.; Lin, Y.; Liu, H.; Anwar, J.; Zhang, J. CD-MOFs Crystal Transformation from Dense to Highly Porous Form for Efficient Drug Loading. *Cryst. Growth Des.* **2019**, *19* , 3888–3894. https://doi.org/10.1021/acs.cgd.9b00319.

8. Pichon, A.; Lazuen-Garay, A.; James, S. L. Solvent-Free Synthesis of a Microporous Metal–Organic Framework. *CrystEngComm* **2006**, *8* , 211. https://doi.org/10.1039/b513750k.

9. Liu, B.; He, Y.; Han, L.; Singh, V.; Xu, X.; Guo, T.; Meng, F.; Xu, X.; York, P.; Liu, Z.; Zhang, J. Microwave-Assisted Rapid Synthesis of γ-Cyclodextrin Metal–Organic Frameworks for Size Control and Efficient Drug Loading. *Cryst. Growth Des* **2017**, *17*, 1654–1660. https://doi.org/10.1021/acs.cgd.6b01658.

10. Schlesinger, M.; Schulze, S.; Hietschold, M.; Mehring, M. Evaluation of Synthetic Methods for Microporous Metal–Organic Frameworks Exemplified by the Competitive Formation of [Cu2(Btc)3(H2O)3] and [Cu2(Btc)(OH)(H2O)]. *Microporous Mesoporous Mater.* **2010**, *132*, 121–127. https://doi.org/10.1016/j.micromeso.2010.02.008.

11. Aiyappa, H. B.; Saha, S.; Garai, B.; Thote, J.; Kurungot, S.; Banerjee, R. A Distinctive PdCl2-Mediated Transformation of Fe-Based Metallogels into Metal–Organic Frameworks. *Cryst. Growth Des* **2014**, *14*, 3434–3437. https://doi.org/10.1021/cg500368q.

12. Banerjee, D.; Finkelstein, J.; Smirnov, A.; Forster, P. M.; Borkowski, L. A.; Teat, S. J.; Parise, J. B. Synthesis and Structural Characterization of Magnesium Based Coordination Networks in Different Solvents. *Cryst. Growth Des* **2011**, *11*, 2572–2579. https://doi.org/10.1021/cg200327y.

13. Luo, L.; Lv, G.-C.; Wang, P.; Liu, Q.; Chen, K.; Sun, W.-Y. PH-Dependent Cobalt(Ii) Frameworks with Mixed 3,3′,5,5′-Tetra(1H-Imidazol-1-Yl)-1,1′-Biphenyl and 1,3,5-Benzenetricarboxylate Ligands: Synthesis, Structure and Sorption Property. *CrystEngComm* **2013**, *15* , 9537. https://doi.org/10.1039/c3ce41056k.

14. Liu, X.; Li, Y.; Ban, Y.; Peng, Y.; Jin, H.; Bux, H.; Xu, L.; Caro, J.; Yang, W. Improvement of Hydrothermal Stability of Zeolitic Imidazolate Frameworks. *Chem. Commun.***2013**, *49*, 9140. https://doi.org/10.1039/c3cc45308a.

15. Hirai, K.; Chen, K.; Fukushima, T.; Horike, S.; Kondo, M.; Louvain, N.; Kim, C.; Sakata, Y.; Meilikhov, M.; Sakata, O.; Kitagawa, S.; Furukawa, S. Programmed Crystallization via Epitaxial Growth and Ligand Replacement towards Hybridizing Porous Coordination Polymer Crystals. *Dalton Trans.* **2013**, *42*, *15868*. https://doi.org/10.1039/c3dt50679g.

16. Furukawa, S.; Hirai, K.; Nakagawa, K.; Takashima, Y.; Matsuda, R.; Tsuruoka, T.; Kondo, M.; Haruki, R.; Tanaka, D.; Sakamoto, H.; Shimomura, S.; Sakata, O.; Kitagawa, S. Heterogeneously Hybridized Porous Coordination Polymer Crystals: Fabrication of Heterometallic Core-Shell Single Crystals with an In-Plane Rotational Epitaxial Relationship. *Angew. Chem., Int. Ed.***2009**, *48* , 1766–1770. https://doi.org/10.1002/anie.200804836.

17. Ockwig, N. W.; Delgado-Friedrichs, O.; O'Keeffe, M.; Yaghi, O. M. Reticular Chemistry: Occurrence and Taxonomy of Nets and Grammar for the Design of Frameworks. *Acc. Chem. Res.* **2005**, *38*, 176–182. https://doi.org/10.1021/ar020022l.

18. O'Keeffe, M.; Peskov, M. A.; Ramsden, S. J.; Yaghi, O. M. The Reticular Chemistry Structure Resource (RCSR) Database Of, and Symbols For, Crystal Nets. *Acc. Chem. Res* **2008**, *41*, 1782–1789. https://doi.org/10.1021/ar800124u.

19. Dinnebier, R. E.; Billinge, S. J. Chapter 1. Principles of Powder Diffraction. *Acc. Chem. Res* **2008**, 1–19.

20. Egerton, R. F. *Physical principles of electron microscopy: An introduction to TEM, Sem, and Aem;* Springer: New York, NY, **2008**.

21. Baati, T.; Njim, L.; Neffati, F.; Kerkeni, A.; Bouttemi, M.; Gref, R.; Najjar, M. F.; Zakhama, A.; Couvreur, P.; Serre, C.; Horcajada, P. In Depth Analysis of the in Vivo Toxicity of Nanoparticles of Porous Iron (Iii) Metal–Organic Frameworks. *Chem. Sci.* **2013**, *4*, 1597. https://doi.org/10.1039/c3sc22116d.

22. Pati, R.; Mehta, R. K.; Mohanty, S.; Padhi, A.; Sengupta, M.; Vaseeharan, B.; Goswami, C.; Sonawane, A. Topical Application of Zinc Oxide Nanoparticles Reduces Bacterial Skin Infection in Mice and Exhibits Antibacterial Activity by Inducing Oxidative Stress Response and Cell Membrane Disintegration in Macrophages. *Nanotechnol. Biol. Med.* **2014**, *10*, 1195–1208. https://doi.org/10.1016/j.nano.2014.02.012.

23. Noro, S.; Kitagawa, S.; Kondo, M.; Seki, K. A New, Methane Adsorbent, Porous Coordination Polymer [{CuSiF6(4,4′-Bipyridine)2}N]. *Angew. Chem. Int. Ed. A.* **2000**, *39* , 2081–2084. https://doi.org/3.0.co;2-a">10.1002/1521-3773(20000616)39:12<2081::aid-anie2081>3.0.co;2-a.

24. Mohideen, H.; Infas, M. Novel metal organic frameworks : synthesis, characterisation and functions http://hdl.handle.net/10023/1892 (accessed Dec 11, **2021**).

25. Jain, P.; Ramachandran, V.; Clark, R. J.; Zhou, H. D.; Toby, B. H.; Dalal, N. S.; Kroto, H. W.; Cheetham, A. K. Multiferroic Behavior Associated with an Order−Disorder Hydrogen Bonding Transition in Metal−Organic Frameworks (MOFs) with the Perovskite ABX3 Architecture. *J. Am. Chem. Soc.* **2009**, *131* , 13625–13627. https://doi.org/10.1021/ja904156s.

26. Rocha, J.; Carlos, L. D.; Paz, F. A. A.; Ananias, D. Luminescent Multifunctional Lanthanides-Based Metal–Organic Frameworks. *Chem. Soc. Rev.* **2011**, *40* , 926–940. https://doi.org/10.1039/c0cs00130a.

27. Harbuzaru, Bogdan V.; Corma, A.; Rey, F.; Jordá, Jose L.; Ananias, D.; Carlos, Luis D.; Rocha, J. A Miniaturized Linear PH Sensor Based on a Highly Photoluminescent Self-Assembled Europium(III) Metal-Organic Framework. *Angew. Chem., Int. Ed.* **2009**, *48* , 6476–6479. https://doi.org/10.1002/anie.200902045.

28. Deep, A.; Bhardwaj, S. K.; Paul, A. K.; Kim, K.-H.; Kumar, P. Surface Assembly of Nano-Metal Organic Framework on Amine Functionalized Indium Tin Oxide Substrate for Impedimetric Sensing of Parathion. *Biosens. Bioelectron.* **2015**, *65*, 226–231. https://doi.org/10.1016/j.bios.2014.10.045.

29. Xu, J.; Shimakoshi, H.; Hisaeda, Y. Development of Metal-Organic Framework (MOF)-B12 System as New Bio-Inspired Heterogeneous Catalyst. *J. Organomet. Chem.* **2015**, 782, 89–95. https://doi.org/10.1016/j.jorganchem.2014.11.015.

30. Díaz, R.; Orcajo, M. G.; Botas, J. A.; Calleja, G.; Palma, J. Co8-MOF-5 as Electrode for Supercapacitors. *Mater. Lett.* **2012**, *68*, 126–128. https://doi.org/10.1016/j.matlet.2011.10.046.

31. Lee, D. Y.; Yoon, S. J.; Shrestha, N. K.; Lee, S.-H.; Ahn, H.; Han, S.-H. Unusual Energy Storage and Charge Retention in Co-Based Metal–Organic-Frameworks. *Microporous Mesoporous Mater.* **2012**, *153*, 163–165. https://doi.org/10.1016/j.micromeso.2011.12.040.

32. McKinlay, Alistair C.; Morris, Russell E.; Horcajada, P.; Férey, G.; Gref, R.; Couvreur, P.; Serre, C. BioMOFs: Metal-Organic Frameworks for Biological and Medical Applications. *Angew. Chem. Int. Ed. A.* **2010**, *49*, 6260–6266. https://doi.org/10.1002/anie.201000048.

33. Zhuang, J.; Kuo, C.-H.; Chou, L.-Y.; Liu, D.-Y.; Weerapana, E.; Tsung, C.-K. Optimized Metal–Organic-Framework Nanospheres for Drug Delivery: Evaluation of Small-Molecule Encapsulation. *ACS Nano* **2014**, *8*, 2812–2819. https://doi.org/10.1021/nn406590q.

34. Babarao, R.; Jiang, J. Unraveling the Energetics and Dynamics of Ibuprofen in Mesoporous Metal−Organic Frameworks. *J. Phys. Chem.***2009**, *113*, 18287–18291. https://doi.org/10.1021/jp906429s.

35.

Pisklak, T. J.; Macías, M.; Coutinho, D. H.; Huang, R. S.; Balkus, K. J. Hybrid Materials for Immobilization of MP-11 Catalyst. *Top. Catal.* **2006**, *38*, 269–278. https://doi.org/10.1007/s11244-006-0025-6.

36. Liu, W.-L.; Lo, S.-H.; Singco, B.; Yang, C.-C.; Huang, H.-Y.; Lin, C.-H. Novel Trypsin–FITC@MOF Bioreactor Efficiently Catalyzes Protein Digestion. *J. Mater. Chem. B* **2013**, *1* , 928. https://doi.org/10.1039/c3tb00257h.

37. Liu, W.-L.; Wu, C.-Y.; Chen, C.-Y.; Singco, B.; Lin, C.-H.; Huang, H.-Y. Fast Multipoint Immobilized MOF Bioreactor. *Chem. Eur. J.* **2014**, n/a-n/a. https://doi.org/10.1002/chem.201400270.

38. Ma, W.; Jiang, Q.; Yu, P.; Yang, L.; Mao, L. Zeolitic Imidazolate Framework-Based Electrochemical Biosensor for in Vivo Electrochemical Measurements. *Anal. Chem.* **2013**, *85* , 7550–7557. https://doi.org/10.1021/ac401576u.

39. Peng, S.; Bie, B.; Sun, Y.; Liu, M.; Cong, H.; Zhou, W.; Xia, Y.; Tang, H.; Deng, H.; Zhou, X. Metal-Organic Frameworks for Precise Inclusion of Single-Stranded DNA and Transfection in Immune Cells. *Nat. Commun.* **2018**, *9* . https://doi.org/10.1038/s41467-018-03650-w.

40. Wu, X.; Ge, J.; Yang, C.; Hou, M.; Liu, Z. Facile Synthesis of Multiple Enzyme-Containing Metal–Organic Frameworks in a Biomolecule-Friendly Environment. *Chem. Commun.* **2015**, *51* , 13408–13411. https://doi.org/10.1039/c5cc05136c.

41. Hou, C.; Wang, Y.; Ding, Q.; Jiang, L.; Li, M.; Zhu, W.; Pan, D.; Zhu, H.; Liu, M. Facile Synthesis of Enzyme-Embedded Magnetic Metal–Organic Frameworks as a Reusable Mimic Multi-Enzyme System: Mimetic Peroxidase Properties and Colorimetric Sensor. *Nanoscale* **2015**, *7* , 18770–18779. https://doi.org/10.1039/c5nr04994f.

42. Lykourinou, V.; Chen, Y.; Wang, X.-S.; Meng, L.; Hoang, T.; Ming, L.-J.; Musselman, R. L.; Ma, S. Immobilization of MP-11 into a Mesoporous Metal–Organic Framework, MP-11@MesoMOF: A New Platform for Enzymatic Catalysis. *J. Am. Chem. Soc.* **2011**, *133* , 10382–10385. https://doi.org/10.1021/ja2038003.

43. Chen, Y.; Lykourinou, V.; Vetromile, C.; Hoang, T.; Ming, L.-J.; Larsen, R. W.; Ma, S. How Can Proteins Enter the Interior of a MOF? Investigation of Cytochrome c Translocation into a MOF Consisting of Mesoporous Cages with Microporous Windows. *J. Am. Chem. Soc.* **2012**, *134*, 13188–13191. https://doi.org/10.1021/ja305144x.

44. Feng, D.; Liu, T.-F.; Su, J.; Bosch, M.; Wei, Z.; Wan, W.; Yuan, D.; Chen, Y.-P.; Wang, X.; Wang, K.; Lian, X.; Gu, Z.-Y.; Park, J.; Zou, X.; Zhou, H.-C. Stable Metal-Organic Frameworks Containing Single-Molecule Traps for Enzyme Encapsulation. *Nat. Commun.* **2015**, *6* . https://doi.org/10.1038/ncomms6979.

45. Wang, Z.; Cohen, S. M. Postsynthetic Modification of Metal–Organic Frameworks. *Chem. Soc. Rev.* **2009**, *38* , 1315. https://doi.org/10.1039/b802258p.

46. Jung, S.; Kim, Y.; Kim, S.-J.; Kwon, T.-H.; Huh, S.; Park, S. Bio-Functionalization of Metal–Organic Frameworks by Covalent Protein Conjugation. *Chem. Commun.* **2011**, *47* , 2904. https://doi.org/10.1039/c0cc03288c.

47. Shih, Y.-H.; Lo, S.-H.; Yang, N.-S.; Singco, B.; Cheng, Y.-J.; Wu, C.-Y.; Chang, I-Hsin.; Huang, H.-Y.; Lin, C.-H. Trypsin-Immobilized Metal-Organic Framework as a Biocatalyst in Proteomics Analysis. *ChemPlusChem* **2012**, *77* , 982–986. https://doi.org/10.1002/cplu.201200186.

48. Morris, W.; Briley, W. E.; Auyeung, E.; Cabezas, M. D.; Mirkin, C. A. Nucleic Acid–Metal Organic Framework (MOF) Nanoparticle Conjugates. *J. Am. Chem. Soc.* **2014**, *136* , 7261–7264. https://doi.org/10.1021/ja503215w.

49. Wang, S.; McGuirk, C. M.; Ross, M. B.; Wang, S.; Chen, P.; Xing, H.; Liu, Y.; Mirkin, C. A. General and Direct Method for Preparing Oligonucleotide-Functionalized Metal–Organic Framework Nanoparticles. *J. Am. Chem. Soc.* **2017**, *139* , 9827–9830. https://doi.org/10.1021/jacs.7b05633.

50. Sun, Y.; Sun, L.; Feng, D.; Zhou, H. An in Situ One-Pot Synthetic Approach towards Multivariate Zirconium MOFs. *Angew. Chem. Int. Ed. A.* **2016**, *55* , 6471–6475. https://doi.org/10.1002/anie.201602274.

51. Verma, S.; Mishra, A. K.; Kumar, J. The Many Facets of Adenine: Coordination, Crystal Patterns, and Catalysis. *Acc. Chem. Res* **2009**, *43* , 79–91. https://doi.org/10.1021/ar9001334.

52. An, J.; Geib, S. J.; Rosi, N. L. Cation-Triggered Drug Release from a Porous Zinc−Adeninate Metal−Organic Framework. *J. Am. Chem. Soc.* **2009**, *131* , 8376–8377. https://doi.org/10.1021/ja902972w.

53. Wu, X.; Ge, J.; Yang, C.; Hou, M.; Liu, Z. Facile Synthesis of Multiple Enzyme-Containing Metal–Organic Frameworks in a Biomolecule-Friendly Environment. *Chem. Commun.* **2015**, *51* , 13408–13411. https://doi.org/10.1039/c5cc05136c.

54. Vassaki, M.; Papathanasiou, K. E.; Hadjicharalambous, C.; Chandrinou, D.; Turhanen, P.; Choquesillo-Lazarte, D.; Demadis, K. D. Self-Sacrificial MOFs for Ultra-Long Controlled Release of Bisphosphonate Anti-Osteoporotic Drugs. *Chem. Commun.***2020**, *56* , 5166–5169. https://doi.org/10.1039/d0cc00439a.

55. Javanbakht, S.; Nezhad-Mokhtari, P.; Shaabani, A.; Arsalani, N.; Ghorbani, M. Incorporating Cu-Based Metal-Organic Framework/Drug Nanohybrids into Gelatin Microsphere for Ibuprofen Oral Delivery. *Mater. Sci. Eng. C* . **2019**, *96*, 302–309. https://doi.org/10.1016/j.msec.2018.11.028.

56. Morris, W.; Briley, W. E.; Auyeung, E.; Cabezas, M. D.; Mirkin, C. A. Nucleic Acid–Metal Organic Framework (MOF) Nanoparticle Conjugates. *J. Am. Chem. Soc.* **2014**, *136* , 7261–7264. https://doi.org/10.1021/ja503215w.

57. Cao, S.-L.; Yue, D.-M.; Li, X.-H.; Smith, T. J.; Li, N.; Zong, M.-H.; Wu, H.; Ma, Y.-Z.; Lou, W.-Y. Novel Nano-/Micro-Biocatalyst: Soybean Epoxide Hydrolase Immobilized on UiO-66-NH2 MOF for Efficient Biosynthesis of Enantiopure (R)-1, 2-Octanediol in Deep Eutectic Solvents. *ACS Sustain. Chem. Eng.* **2016**, *4*, 3586–3595. https://doi.org/10.1021/acssuschemeng.6b00777.

58. Nel, A. E.; Parak, W. J.; Chan, W. C. W.; Xia, T.; Hersam, M. C.; Brinker, C. J.; Zink, J. I.; Pinkerton, K. E.; Baer, D. R.; Weiss, P. S. Where Are We Heading in Nanotechnology Environmental Health and Safety and Materials Characterization? *ACS Nano* **2015**, *9* , 5627–5630. https://doi.org/10.1021/acsnano.5b03496.

59. Rojas, S.; Devic, T.; Horcajada, P. Metal Organic Frameworks Based on Bioactive Components. *J. Mater. Chem. B* **2017**, *5* , 2560–2573. https://doi.org/10.1039/c6tb03217f.

60. Horcajada, P.; Gref, R.; Baati, T.; Allan, P. K.; Maurin, G.; Couvreur, P.; Férey, G.; Morris, R. E.; Serre, C. Metal–Organic Frameworks in Biomedicine. *Chem. Rev.* **2011**, *112* , 1232–1268. https://doi.org/10.1021/cr200256v.

61. Dongmei, L.; Zhiwei, W.; Qi, Z.; Fuyi, C.; Yujuan, S.; Xiaodong, L. Drinking Water Toxicity Study of the Environmental Contaminant—Bromate. *Regul. Toxicol. Pharmacol* **2015**, *73* , 802–810. https://doi.org/10.1016/j.yrtph.2015.10.015.

62. Leng, X.; Dong, X.; Wang, W.; Sai, N.; Yang, C.; You, L.; Huang, H.; Yin, X.; Ni, J. Biocompatible Fe-Based Micropore Metal-Organic Frameworks as Sustained-Release Anticancer Drug Carriers. *Molecules* **2018**, *23*, 2490. https://doi.org/10.3390/molecules23102490.

63. Gao, X.; Cui, R.; Song, L.; Liu, Z. Hollow Structural Metal–Organic Frameworks Exhibit High Drug Loading Capacity, Targeted Delivery and Magnetic Resonance/Optical Multimodal Imaging. *Dalton Trans.* **2019**, *48* , 17291–17297. https://doi.org/10.1039/c9dt03287h.

64. Zhang, M.; Chen, Y.-P.; Bosch, M.; Gentle, T.; Wang, K.; Feng, D.; Wang, Z. U.; Zhou, H.-C. Symmetry-Guided Synthesis of Highly Porous Metal-Organic Frameworks with Fluorite Topology. *Acc. Chem. Res* **2013**, *53*, 815–818. https://doi.org/10.1002/anie.201307340.

65. Abánades Lázaro, I.; Abánades Lázaro, S.; Forgan, R. S. Enhancing Anticancer Cytotoxicity through Bimodal Drug Delivery from Ultrasmall Zr MOF Nanoparticles. *Chem. Commun.* **2018**, *54* , 2792–2795. https://doi.org/10.1039/c7cc09739e.

66. He, Y.; Zhang, W.; Guo, T.; Zhang, G.; Qin, W.; Zhang, L.; Wang, C.; Zhu, W.; Yang, M.; Hu, X.; Singh, V.; Wu, L.; Gref, R.; Zhang, J. Drug Nanoclusters Formed in Confined Nano-Cages of CD-MOF: Dramatic Enhancement of Solubility and Bioavailability of Azilsartan. *Acta Pharm. Sin. B.* **2019**, *9*, 97–106. https://doi.org/10.1016/j.apsb.2018.09.003.

67. Inoue, Y.; Nanri, A.; Murata, I.; Kanamoto, I. Characterization of Inclusion Complex of Coenzyme Q10 with the New Carrier CD-MOF-1 Prepared by Solvent Evaporation. *AAPS PharmSciTech* **2018**, *19* , 3048–3056. https://doi.org/10.1208/s12249-018-1136-7.

68. Schnabel, J.; Ettlinger, R.; Bunzen, H. Zn-MOF-74 as PH-Responsive Drug-Delivery System of Arsenic Trioxide. *ChemNanoMat* **2020**, *6* , 1229–1236. https://doi.org/10.1002/cnma.202000221.

69. Alsaiari, S. K.; Patil, S.; Alyami, M.; Alamoudi, K. O.; Aleisa, F. A.; Merzaban, J. S.; Li, M.; Khashab, N. M. Endosomal Escape and Delivery of CRISPR/Cas9 Genome Editing Machinery Enabled by Nanoscale Zeolitic Imidazolate Framework. *J. Am. Chem. Soc.* **2017**, *140* , 143–146. https://doi.org/10.1021/jacs.7b11754.

70. Horcajada, P.; Gref, R.; Baati, T.; Allan, P. K.; Maurin, G.; Couvreur, P.; Férey, G.; Morris, R. E.; Serre, C. Metal–Organic Frameworks in Biomedicine. *Chem. Rev.* **2011**, *112* , 1232–1268. https://doi.org/10.1021/cr200256v.

71. Horcajada, P.; Chalati, T.; Serre, C.; Gillet, B.; Sebrie, C.; Baati, T.; Eubank, J. F.; Heurtaux, D.; Clayette, P.; Kreuz, C.; Chang, J.-S.; Hwang, Y. K.; Marsaud, V.; Bories, P.-N.; Cynober, L.; Gil, S.; Férey, G.; Couvreur, P.; Gref, R. Porous Metal–Organic-Framework Nanoscale Carriers as a Potential Platform for Drug Delivery and Imaging. *Nat. Mater.* **2009**, *9* , 172–178. https://doi.org/10.1038/nmat2608.

72. Chalati, T.; Horcajada, P.; Couvreur, P.; Serre, C.; Ben Yahia, M.; Maurin, G.; Gref, R. Porous Metal Organic Framework Nanoparticles to Address the Challenges Related to Busulfan Encapsulation. *Nanomedicine* **2011**, *6*, 1683–1695. https://doi.org/10.2217/nnm.11.69.

73. Anand, R.; Borghi, F.; Manoli, F.; Manet, I.; Agostoni, V.; Reschiglian, P.; Gref, R.; Monti, S. Host–Guest Interactions in Fe(III)-Trimesate MOF Nanoparticles Loaded with Doxorubicin. *J. Mater. Chem. B* **2014**, *118*, 8532–8539. https://doi.org/10.1021/jp503809w.

74. Li, X.; Semiramoth, N.; Hall, S.; Tafani, V.; Josse, J.; Laurent, F.; Salzano, G.; Foulkes, D.; Brodin, P.; Majlessi, L.; Ghermani, N.; Maurin, G.; Couvreur, P.; Serre, C.; Bernet-Camard, M.; Zhang, J.; Gref, R. Compartmentalized Encapsulation of Two Antibiotics in Porous Nanoparticles: An Efficient Strategy to Treat Intracellular Infections. *Part. Part. Syst. Charact.* **2019**, *36*, 1800360. https://doi.org/10.1002/ppsc.201800360.

75. Agostoni, V.; Chalati, T.; Horcajada, P.; Willaime, H.; Anand, R.; Semiramoth, N.; Baati, T.; Hall, S.; Maurin, G.; Chacun, H.; Bouchemal, K.; Martineau, C.; Taulelle, F.; Couvreur, P.; Rogez-Kreuz, C.; Clayette, P.; Monti, S.; Serre, C.; Gref, R. Towards an Improved Anti-HIV Activity of NRTI via Metal-Organic Frameworks Nanoparticles. *Adv. Healthc. Mater.* **2013**, *2* , 1630–1637. https://doi.org/10.1002/adhm.201200454.

76. Agostoni, V.; Anand, R.; Monti, S.; Hall, S.; Maurin, G.; Horcajada, P.; Serre, C.; Bouchemal, K.; Gref, R. Impact of Phosphorylation on the Encapsulation of Nucleoside Analogues within Porous Iron(Iii) Metal–Organic Framework MIL-100(Fe) Nanoparticles. *J. Mater. Chem. B* **2013**, *1*, 4231. https://doi.org/10.1039/c3tb20653j.

77. Marcos-Almaraz, M. T.; Gref, R.; Agostoni, V.; Kreuz, C.; Clayette, P.; Serre, C.; Couvreur, P.; Horcajada, P. Towards Improved HIV-Microbicide Activity through the Co-Encapsulation of NRTI Drugs in Biocompatible Metal Organic Framework Nanocarriers. *J. Mater. Chem. B* **2017**, *5* , 8563–8569. https://doi.org/10.1039/c7tb01933e.

78. He, Y.; Zhang, W.; Guo, T.; Zhang, G.; Qin, W.; Zhang, L.; Wang, C.; Zhu, W.; Yang, M.; Hu, X.; Singh, V.; Wu, L.; Gref, R.; Zhang, J. Drug Nanoclusters Formed in Confined Nano-Cages of CD-MOF: Dramatic Enhancement of Solubility and Bioavailability of Azilsartan. *Acta Pharm. Sin. B* **2019**, *9* , 97–106. https://doi.org/10.1016/j.apsb.2018.09.003.

79. Horcajada, P.; Serre, C.; Maurin, G.; Ramsahye, N. A.; Balas, F.; Vallet-RegíM.; Sebban, M.; Taulelle, F.; FéreyG. Flexible Porous Metal-Organic Frameworks for a Controlled Drug Delivery. *J. Am. Chem. Soc.* **2008**, *130*, 6774–6780. https://doi.org/10.1021/ja710973k.

80. Rojas, S.; Carmona, F. J.; Maldonado, C. R.; Horcajada, P.; Hidalgo, T.; Serre, C.; Navarro, J. A. R.; Barea, E. Nanoscaled Zinc Pyrazolate Metal–Organic Frameworks as Drug-Delivery Systems. *Inorg. Chem.* **2016**, *55* , 2650–2663. https://doi.org/10.1021/acs.inorgchem.6b00045.

81. Bag, P. P.; Wang, D.; Chen, Z.; Cao, R. Outstanding Drug Loading Capacity by Water Stable Microporous MOF: A Potential Drug Carrier. *Chem. Commun.* **2016**, *52* , 3669–3672. https://doi.org/10.1039/c5cc09925k.

82. Li, Z.; Guo, R.; Gu, Z.; Wang, X.; Wang, Y.; Xu, H.; Wang, C.; Liu, X. Identification of a Promoter Element Mediating Kisspeptin-Induced Increases in GnRH Gene Expression in Sheep. *Gene* **2019**, *699*, 1–7. https://doi.org/10.1016/j.gene.2019.03.006.

83. Li, X.; Guo, T.; Lachmanski, L.; Manoli, F.; Menendez-Miranda, M.; Manet, I.; Guo, Z.; Wu, L.; Zhang, J.; Gref, R. Cyclodextrin-Based Metal-Organic Frameworks Particles as Efficient Carriers for Lansoprazole: Study of Morphology and Chemical Composition of Individual Particles. *Int. J. Pharm.* **2017**, *531*, 424–432. https://doi.org/10.1016/j.ijpharm.2017.05.056.

84. Hu, X.; Wang, C.; Wang, L.; Liu, Z.; Wu, L.; Zhang, G.; Yu, L.; Ren, X.; York, P.; Sun, L.; Zhang, J.; Li, H. Nanoporous CD-MOF Particles with Uniform and Inhalable Size for Pulmonary Delivery of Budesonide. *Int. J. Pharm.* **2019**, *564*, 153–161.https://doi.org/10.1016/j.ijpharm.2019.04.030.
`

85. Sun, K.; Li, L.; Yu, X.; Liu, L.; Meng, Q.; Wang, F.; Zhang, R. Functionalization of Mixed Ligand Metal-Organic Frameworks as the Transport Vehicles for DrugsJ. *Colloid Interface Sci.* **2017**, *486*, 128–135. https://doi.org/10.1016/j.jcis.2016.09.068.

86. Simon, M. A.; Anggraeni, E.; Soetaredjo, F. E.; Santoso, S. P.; Irawaty, W.; Thanh, T. C.; Hartono, S. B.; Yuliana, M.; Ismadji, S. Hydrothermal Synthesize of HF-Free MIL-100(Fe) for Isoniazid-Drug Delivery. *Sci. Rep.* **2019**, *9* . https://doi.org/10.1038/s41598-019-53436-3.

87. Taherzade, S.; Soleimannejad, J.; Tarlani, A. Application of Metal-Organic Framework Nano-MIL-100(Fe) for Sustainable Release of Doxycycline and Tetracycline. *Nanomaterials* **2017**, *7* , 215. https://doi.org/10.3390/nano7080215.

88. Rezaei, M.; Abbasi, A.; Varshochian, R.; Dinarvand, R.; Jeddi-Tehrani, M. NanoMIL-100(Fe) Containing Docetaxel for Breast Cancer Therapy. *Artif. Cells Nanomed. Biotechnol* **2017**, *46*, 1390–1401. https://doi.org/10.1080/21691401.2017.1369425.

89. Taylor-Pashow, K. M. L.; Della Rocca, J.; Xie, Z.; Tran, S.; Lin, W. Postsynthetic Modifications of Iron-Carboxylate Nanoscale Metal−Organic Frameworks for Imaging and Drug Delivery. *J. Am. Chem. Soc.* **2009**, *131* , 14261–14263. https://doi.org/10.1021/ja906198y.

Cunha, D.; Ben Yahia, M.; Hall, S.; Miller, S. R.; Chevreau, H.; Elkaïm, E.; Maurin, G.; Horcajada, P.; Serre, C. Rationale of Drug Encapsulation and Release from Biocompatible Porous Metal–Organic Frameworks. *Chem. Mater.* **2013**, *25* , 2767–2776. https://doi.org/10.1021/cm400798p.

90. Sun, C.-Y.; Qin, C.; Wang, C.-G.; Su, Z.-M.; Wang, S.; Wang, X.-L.; Yang, G.-S.; Shao, K.-Z.; Lan, Y.-Q.; Wang, E.-B. Chiral Nanoporous Metal-Organic Frameworks with High Porosity as Materials for Drug Delivery. *Adv. Mater.* **2011**, *23*, 5629–5632. https://doi.org/10.1002/adma.201102538.

91. Oh, H.; Li, T.; An, J. Drug Release Properties of a Series of Adenine-Based Metal-Organic Frameworks. *Chem. Eur. J.* **2015**, *21* , 17010–17015. https://doi.org/10.1002/chem.201501560.

92. Sun, C.-Y.; Qin, C.; Wang, X.-L.; Yang, G.-S.; Shao, K.-Z.; Lan, Y.-Q.; Su, Z.-M.; Huang, P.; Wang, C.-G.; Wang, E.-B. Zeolitic Imidazolate Framework-8 as Efficient PH-Sensitive Drug Delivery Vehicle. *Dalton Trans.* **2012**, *41*, 6906. https://doi.org/10.1039/c2dt30357d.

93. Gao, H.; Zhang, Y.; Chi, B.; Lin, C.; Tian, F.; Xu, M.; Wang, Y.; Xu, Z.; Li, L.; Wang, J. Synthesis of "Dual-Key-And-Lock" Drug Carriers for Imaging and Improved Drug Release. *Nanotechnology* **2020**, *31* , 445102. https://doi.org/10.1088/1361-6528/aba65a.

94. He, C.; Lu, K.; Liu, D.; Lin, W. Nanoscale Metal–Organic Frameworks for the Co-Delivery of Cisplatin and Pooled SiRNAs to Enhance Therapeutic Efficacy in Drug-Resistant Ovarian Cancer Cells. *J. Am. Chem. Soc.* **2014**, *136* , 5181–5184. https://doi.org/10.1021/ja4098862.

95. Zhang, W.; Yu, S.; Zhang, S.; Zhou, J.; Ning, S.; Wang, X.; Wei, Y. Separation of Scandium from the Other Rare Earth Elements with a Novel Macro-Porous Silica-Polymer Based Adsorbent HDEHP/SiO2-P. *Hydrometallurgy* **2019**, *185*, 117–124. https://doi.org/10.1016/j.hydromet.2019.01.012.

96. Férey, G.; Mellot-Draznieks, C.; Serre, C.; Millange, F. Crystallized Frameworks with Giant Pores: Are There Limits to the Possible? *Acc. Chem. Res.* **2005**, *38* , 217–225. https://doi.org/10.1021/ar040163i.

97. Horcajada, P.; Serre, C.; Vallet-Regí, M.; Sebban, M.; Taulelle, F.; Férey, G. Metal–Organic Frameworks as Efficient Materials for Drug Delivery. *Angew. Chem. Int. Ed.* **2006**, *45*, 5974–5978. https://doi.org/10.1002/anie.200601878.

98. Xing, K.; Fan, R.; Wang, F.; Nie, H.; Du, X.; Gai, S.; Wang, P.; Yang, Y. Dual-Stimulus-Triggered Programmable Drug Release and Luminescent Ratiometric PH Sensing from Chemically Stable Biocompatible Zinc Metal–Organic Framework. *ACS Appl. Mater. Interfaces* **2018**, *10* , 22746–22756. https://doi.org/10.1021/acsami.8b06270.

99. Zheng, H.; Zhang, Y.; Liu, L.; Wan, W.; Guo, P.; Nyström, A. M.; Zou, X. One-Pot Synthesis of Metal–Organic Frameworks with Encapsulated Target Molecules and Their Applications for Controlled Drug Delivery. *J. Am. Chem. Soc.* **2016**, *138*, 962–968. https://doi.org/10.1021/jacs.5b11720.

100. Wu, Q.; Niu, M.; Chen, X.; Tan, L.; Fu, C.; Ren, X.; Ren, J.; Li, L.; Xu, K.; Zhong, H.; Meng, X. Biocompatible and Biodegradable Zeolitic Imidazolate Framework/Polydopamine Nanocarriers for Dual Stimulus Triggered Tumor Thermo-Chemotherapy. *Biomaterials* **2018**, *162*, 132–143. https://doi.org/10.1016/j.biomaterials.2018.02.022.

101. Sun, Q.; Bi, H.; Wang, Z.; Li, C.; Wang, X.; Xu, J.; Zhu, H.; Zhao, R.; He, F.; Gai, S.; Yang, P. Hyaluronic Acid-Targeted and PH-Responsive Drug Delivery System Based on Metal-Organic Frameworks for Efficient Antitumor Therapy. *Biomaterials* **2019**, *223*, 119473. https://doi.org/10.1016/j.biomaterials.2019.119473.

102. Lee, D. B. N.; Roberts, M.; Bluchel, C. G.; Odell, R. A. Zirconium: Biomedical and Nephrological Applications. *ASAIO J.* **2010**, *56* , 550–556. https://doi.org/10.1097/mat.0b013e3181e73f20.

103. Abánades Lázaro, I.; Haddad, S.; Rodrigo-Muñoz, J. M.; Marshall, R. J.; Sastre, B.; del Pozo, V.; Fairen-Jimenez, D.; Forgan, R. S. Surface-Functionalization of Zr-Fumarate MOF for Selective Cytotoxicity and Immune System Compatibility in Nanoscale Drug Delivery. *ACS Appl. Mater. Interfaces* **2018**, *10* , 31146–31157. https://doi.org/10.1021/acsami.8b11652.

104. Smaldone, R. A.; Forgan, R. S.; Furukawa, H.; Gassensmith, J. J.; Slawin, A. M. Z.; Yaghi, O. M.; Stoddart, J. F. Metal-Organic Frameworks from Edible Natural Products. *Angew. Chem. Int. Ed.* **2010**, *49* , 8630–8634. https://doi.org/10.1002/anie.201002343.

105. Han, Y.; Liu, W.; Huang, J.; Qiu, S.; Zhong, H.; Liu, D.; Liu, J. Cyclodextrin-Based Metal-Organic Frameworks (CD-MOFs) in Pharmaceutics and Biomedicine. *Pharmaceutics* **2018**, *10* , 271. https://doi.org/10.3390/pharmaceutics10040271.

106. He, Y.; Xu, J.; Sun, X.; Ren, X.; Maharjan, A.; York, P.; Su, Y.; Li, H.; Zhang, J. Cuboidal Tethered Cyclodextrin Frameworks Tailored for Hemostasis and Injured Vessel Targeting. *Theranostics* **2019**, *9* , 2489–2504. https://doi.org/10.7150/thno.31159.

107. McKinlay, Alistair C.; Morris, Russell E.; Horcajada, P.; Férey, G.; Gref, R.; Couvreur, P.; Serre, C. BioMOFs: Metal-Organic Frameworks for Biological and Medical Applications. *Angew. Chem. Int. Ed.* **2010**, *49* , 6260–6266. https://doi.org/10.1002/anie.201000048.

108. Li, Y.; Li, X.; Guan, Q.; Zhang, C.; Xu, T.; Dong, Y.; Bai, X.; Zhang, W. Strategy for Chemotherapeutic Delivery Using a Nanosized Porous Metal-Organic Framework with a Central Composite Design. *Int. J. Nanomedicine* **2017**, *12*, 1465–1474. https://doi.org/10.2147/ijn.s119115.

109. Xiao, J.; Zhu, Y.; Huddleston, S.; Li, P.; Xiao, B.; Farha, O. K.; Ameer, G. A. Copper Metal–Organic Framework Nanoparticles Stabilized with Folic Acid Improve Wound Healing in Diabetes. *ACS Nano* **2018**, *12* , 1023–1032. https://doi.org/10.1021/acsnano.7b01850.

110. Hou, L.; Qin, Y.; Li, J.; Qin, S.; Huang, Y.; Lin, T.; Guo, L.; Ye, F.; Zhao, S. A Ratiometric Multicolor Fluorescence Biosensor for Visual Detection of Alkaline Phosphatase Activity via a Smartphone. *Biosens. Bioelectron.* **2019**, *143*, 111605. https://doi.org/10.1016/j.bios.2019.111605.

111. Jo, J. H.; Kim, H.-C.; Huh, S.; Kim, Y.; Lee, D. N. Antibacterial Activities of Cu-MOFs Containing Glutarates and Bipyridyl Ligands. *Dalton Trans.* **2019**, *48* , 8084–8093. https://doi.org/10.1039/c9dt00791a.

112. Lu, W.; Wei, Z.; Gu, Z.-Y.; Liu, T.-F.; Park, J.; Park, J.; Tian, J.; Zhang, M.; Zhang, Q.; Gentle III, T.; Bosch, M.; Zhou, H.-C. Tuning the Structure and Function of Metal–Organic Frameworks via Linker Design. *Chem. Soc. Rev.* **2014**, *43* , 5561–5593. https://doi.org/10.1039/c4cs00003j.

113. Simon-Yarza, T.; Mielcarek, A.; Couvreur, P.; Serre, C. Nanoparticles of Metal-Organic Frameworks: On the Road to in Vivo Efficacy in Biomedicine. *Adv. Mater.* **2018**, *30* , 1707365. https://doi.org/10.1002/adma.201707365.

114. Bala, S.; Bhattacharya, S.; Goswami, A.; Adhikary, A.; Konar, S.; Mondal, R. Designing Functional Metal–Organic Frameworks by Imparting a Hexanuclear Copper-Based Secondary Building Unit Specific Properties: Structural Correlation with Magnetic and Photocatalytic Activity. *Cryst. Growth Des.* **2014**, *14* , 6391–6398. https://doi.org/10.1021/cg501226v.

115. Giménez-Marqués, M.; Hidalgo, T.; Serre, C.; Horcajada, P. Nanostructured Metal–Organic Frameworks and Their Bio-Related Applications. *Coord. Chem. Rev.* **2016**, *307*, 342–360. https://doi.org/10.1016/j.ccr.2015.08.008.

116. Xu, H.; Cai, J.; Xiang, S.; Zhang, Z.; Wu, C.; Rao, X.; Cui, Y.; Yang, Y.; Krishna, R.; Chen, B.; Qian, G. A Cationic Microporous Metal–Organic Framework for Highly Selective Separation of Small Hydrocarbons at Room Temperature. *J. Mater. Chem. A* **2013**, *1* , 9916. https://doi.org/10.1039/c3ta12086d.

117. Gramaccioli, C. M. The Crystal Structure of Zinc Glutamate Dihydrate. *Acta Crystallogr.* **1966**, *21* , 600–605. https://doi.org/10.1107/s0365110x66003529.

118. Imaz, I.; Rubio-Martínez, M.; An, J.; Solé-Font, I.; Rosi, N. L.; Maspoch, D. Metal–Biomolecule Frameworks (MBioFs). *Chem. Commun.***2011**, *47* , 7287. https://doi.org/10.1039/c1cc11202c.

119. Miller, S. R.; Heurtaux, D.; Baati, T.; Horcajada, P.; Grenèche, J.-M.; Serre, C. Biodegradable Therapeutic MOFs for the Delivery of Bioactive Molecules. *Chem. Commun.***2010**, *46* , 4526. https://doi.org/10.1039/c001181a.

120. Levine, D. J.; Runčevski, T.; Kapelewski, M. T.; Keitz, B. K.; Oktawiec, J.; Reed, D. A.; Mason, J. A.; Jiang, H. Z. H.; Colwell, K. A.; Legendre, C. M.; FitzGerald, S. A.; Long, J. R. Olsalazine-Based Metal–Organic Frameworks as Biocompatible Platforms for H2 Adsorption and Drug Delivery. *J. Am. Chem. Soc.* **2016**, *138* , 10143–10150. https://doi.org/10.1021/jacs.6b03523.

121. Rieter, W. J.; Pott, K. M.; Taylor, K. M. L.; Lin, W. Nanoscale Coordination Polymers for Platinum-Based Anticancer Drug Delivery. *J. Am. Chem. Soc.* **2008**, *130*, 11584–11585. https://doi.org/10.1021/ja803383k.

122. Li, Z.; Zhao, S.; Wang, H.; Peng, Y.; Tan, Z.; Tang, B. Functional Groups Influence and Mechanism Research of UiO-66-Type Metal-Organic Frameworks for Ketoprofen Delivery. *Colloids Surf. B* **2019**, *178*, 1–7. https://doi.org/10.1016/j.colsurfb.2019.02.027.

123. Cavka, J. H.; Jakobsen, S.; Olsbye, U.; Guillou, N.; Lamberti, C.; Bordiga, S.; Lillerud, K. P. A New Zirconium Inorganic Building Brick Forming Metal Organic Frameworks with Exceptional Stability. *J. Am. Chem. Soc.* **2008**, *130* , 13850–13851. https://doi.org/10.1021/ja8057953.

124. Xu, Z.; Li, M.; Li, X.; Liu, X.; Ma, F.; Wu, S.; Yeung, K. W. K.; Han, Y.; Chu, P. K. Antibacterial Activity of Silver Doped Titanate Nanowires on Ti Implants. *ACS Appl. Mater. Interfaces* ***2016***, *8* , 16584–16594. https://doi.org/10.1021/acsami.6b04161.

125. Xu, H.; Zhang, G.; Xu, K.; Wang, L.; Yu, L.; Xing, M. M. Q.; Qiu, X. Mussel-Inspired Dual-Functional PEG Hydrogel Inducing Mineralization and Inhibiting Infection in Maxillary Bone Reconstruction. *Mater. Sci. Eng. C* . **2018**, *90*, 379–386. https://doi.org/10.1016/j.msec.2018.04.066.

126. Lin, S.; Liu, X.; Tan, L.; Cui, Z.; Yang, X.; Yeung, K. W. K.; Pan, H.; Wu, S. Porous Iron-Carboxylate Metal–Organic Framework: A Novel Bioplatform with Sustained Antibacterial Efficacy and Nontoxicity. *ACS Appl. Mater. Interfaces* **2017**, *9* , 19248–19257. https://doi.org/10.1021/acsami.7b04810.

127. Sava Gallis, D. F.; Butler, K. S.; Agola, J. O.; Pearce, C. J.; McBride, A. A. Antibacterial Countermeasures via Metal–Organic Framework-Supported Sustained Therapeutic Release. *ACS Appl. Mater. Interfaces* **2019**, *11* , 7782–7791. https://doi.org/10.1021/acsami.8b21698.

128. Zhang, X.; Liu, L.; Huang, L.; Zhang, W.; Wang, R.; Yue, T.; Sun, J.; Li, G.; Wang, J. The Highly Efficient Elimination of Intracellular Bacteria via a Metal Organic Framework (MOF)-Based Three-In-One Delivery System. *Nanoscale* **2019**, *11* , 9468–9477. https://doi.org/10.1039/c9nr01284b.

129. Guo, A.; Durymanov, M.; Permyakova, A.; Sene, S.; Serre, C.; Reineke, J. Metal Organic Framework (MOF) Particles as Potential Bacteria-Mimicking Delivery Systems for Infectious Diseases: Characterization and Cellular Internalization in Alveolar Macrophages. *Pharm. Res.* **2019**, *36* . https://doi.org/10.1007/s11095-019-2589-4.

130. Yu, M.; You, D.; Zhuang, J.; Lin, S.; Dong, L.; Weng, S.; Zhang, B.; Cheng, K.; Weng, W.; Wang, H. Controlled Release of Naringin in Metal-Organic Framework-Loaded Mineralized Collagen Coating to Simultaneously Enhance Osseointegration and Antibacterial Activity. *ACS Appl. Mater. Interfaces* **2017**, *9* , 19698–19705. https://doi.org/10.1021/acsami.7b05296.

131. Wang, S.; Wang, Y.; Peng, Y.; Yang, X. Exploring the Antibacteria Performance of Multicolor Ag, Au, and Cu Nanoclusters. *ACS Appl. Mater. Interfaces* **2019**, *11*, 8461–8469. https://doi.org/10.1021/acsami.8b22143.

132. Tran, C. D.; Prosenc, F.; Franko, M.; Benzi, G. One-Pot Synthesis of Biocompatible Silver Nanoparticle Composites from Cellulose and Keratin: Characterization and Antimicrobial Activity. *ACS Appl. Mater. Interfaces* **2016**, *8* , 34791–34801. https://doi.org/10.1021/acsami.6b14347.

133. Shakya, S.; He, Y.; Ren, X.; Guo, T.; Maharjan, A.; Luo, T.; Wang, T.; Dhakhwa, R.; Regmi, B.; Li, H.; Gref, R.; Zhang, J. Ultrafine Silver Nanoparticles Embedded in Cyclodextrin Metal-Organic Frameworks with GRGDS Functionalization to Promote Antibacterial and Wound Healing Application. *Small* **2019**, *15* , 1901065. https://doi.org/10.1002/smll.201901065.

134. Yang, Y.; Wu, X.; He, C.; Huang, J.; Yin, S.; Zhou, M.; Ma, L.; Zhao, W.; Qiu, L.; Cheng, C.; Zhao, C. Metal–Organic Framework/Ag-Based Hybrid Nanoagents for Rapid and Synergistic Bacterial Eradication. *ACS Appl. Mater. Interfaces* **2020**, *12* , 13698–13708. https://doi.org/10.1021/acsami.0c01666.

135. Mohamed, N. A.; Davies, R. P.; Lickiss, P. D.; Ahmetaj-Shala, B.; Reed, D. M.; Gashaw, H. H.; Saleem, H.; Freeman, G. R.; George, P. M.; Wort, S. J.; Morales-Cano, D.; Barreira, B.; Tetley, T. D.; Chester, A. H.; Yacoub, M. H.; Kirkby, N. S.; Moreno, L.; Mitchell, J. A. Chemical and Biological Assessment of Metal Organic Frameworks (MOFs) in Pulmonary Cells and in an Acute in Vivo Model: Relevance to Pulmonary Arterial Hypertension Therapy. *Pulm. Circ.* **2017**, *7* , 643–653. https://doi.org/10.1177/2045893217710224.

136. Wyszogrodzka-Gaweł, G.; Dorożyński, P.; Giovagnoli, S.; Strzempek, W.; Pesta, E.; Węglarz, W. P.; Gil, B.; Menaszek, E.; Kulinowski, P. An Inhalable Theranostic System for Local Tuberculosis Treatment Containing an Isoniazid Loaded Metal Organic Framework Fe-MIL-101-NH2—from Raw MOF to Drug Delivery System. *Pharmaceutics* **2019**, *11* , 687. https://doi.org/10.3390/pharmaceutics11120687.

137. Wyszogrodzka, G.; Dorożyński, P.; Gil, B.; Roth, W. J.; Strzempek, M.; Marszałek, B.; Węglarz, W. P.; Menaszek, E.; Strzempek, W.; Kulinowski, P. Iron-Based Metal-Organic Frameworks as a Theranostic Carrier for Local Tuberculosis Therapy. *Pharm. Res.* **2018**, *35* . https://doi.org/10.1007/s11095-018-2425-2.

138. Duan, Y.; Ye, F.; Huang, Y.; Qin, Y.; He, C.; Zhao, S. One-Pot Synthesis of a Metal–Organic Framework-Based Drug Carrier for Intelligent Glucose-Responsive Insulin Delivery. *Chem. Commun.* **2018**, *54* , 5377–5380. https://doi.org/10.1039/c8cc02708k.

139. Yang, X.-X.; Feng, P.; Cao, J.; Liu, W.; Tang, Y. Composition Engineered Metal-Organic-Framework-Based Microneedles for Glucose-Mediated Transdermal Insulin Delivery. *ACS Appl. Mater. Interfaces* **2020**. https://doi.org/10.1021/acsami.9b20774.

140. Kim, S.-N.; Park, C. G.; Huh, B. K.; Lee, S. H.; Min, C. H.; Lee, Y. Y.; Kim, Y. K.; Park, K. H.; Choy, Y. B. Metal-Organic Frameworks, NH2-MIL-88(Fe), as Carriers for Ophthalmic Delivery of Brimonidine. *Acta Biomater.* **2018**, *79*, 344–353. https://doi.org/10.1016/j.actbio.2018.08.023.

141. Gandara-Loe, J.; Souza, B. E.; Missyul, A.; Giraldo, G.; Tan, J.-C. .; Silvestre-Albero, J. MOF-Based Polymeric Nanocomposite Films as Potential Materials for Drug Delivery Devices in Ocular Therapeutics. *ACS Appl. Mater. Interfaces* **2020**, *12* , 30189–30197. https://doi.org/10.1021/acsami.0c07517.

142. Zhang, H.; Jiang, W.; Liu, R.; Zhang, J.; Zhang, D.; Li, Z.; Luan, Y. Rational Design of Metal Organic Framework Nanocarrier-Based Codelivery System of Doxorubicin Hydrochloride/Verapamil Hydrochloride for Overcoming Multidrug Resistance with Efficient Targeted Cancer Therapy. *ACS Appl. Mater. Interfaces* **2017**, *9* , 19687–19697. https://doi.org/10.1021/acsami.7b05142.

143. Zhang, L.; Wang, Z.; Zhang, Y.; Cao, F.; Dong, K.; Ren, J.; Qu, X. Erythrocyte Membrane Cloaked Metal–Organic Framework Nanoparticle as Biomimetic Nanoreactor for Starvation-Activated Colon Cancer Therapy. *ACS Nano* **2018**, *12* , 10201–10211. https://doi.org/10.1021/acsnano.8b05200.

144. Jiang, W.; Zhang, H.; Wu, J.; Zhai, G.; Li, Z.; Luan, Y.; Garg, S. CuS@MOF-Based Well-Designed Quercetin Delivery System for Chemo–Photothermal Therapy. *ACS Appl. Mater. Interfaces* **2018**, *10* , 34513–34523. https://doi.org/10.1021/acsami.8b13487.

145. Huang, J.; Li, N.; Zhang, C.; Meng, Z. Metal–Organic Framework as a Microreactor for in Situ Fabrication of Multifunctional Nanocomposites for Photothermal–Chemotherapy of Tumors in Vivo. *ACS Appl. Mater. Interfaces* **2018**, *10* , 38729–38738. https://doi.org/10.1021/acsami.8b12394.

146. Gao, S.; Zheng, P.; Li, Z.; Feng, X.; Yan, W.; Chen, S.; Guo, W.; Liu, D.; Yang, X.; Wang, S.; Liang, X.-J.; Zhang, J. Biomimetic O2-Evolving Metal-Organic Framework Nanoplatform for Highly Efficient Photodynamic Therapy against Hypoxic Tumor. *Biomaterials* **2018**, *178*, 83–94. https://doi.org/10.1016/j.biomaterials.2018.06.007.

147. Meng, X.; Deng, J.; Liu, F.; Guo, T.; Liu, M.; Dai, P.; Fan, A.; Wang, Z.; Zhao, Y. Triggered All-Active Metal Organic Framework: Ferroptosis Machinery Contributes to the Apoptotic Photodynamic Antitumor Therapy. *Nano Lett.* **2019**, *19* , 7866–7876. https://doi.org/10.1021/acs.nanolett.9b02904.

148. Min, H.; Wang, J.; Qi, Y.; Zhang, Y.; Han, X.; Xu, Y.; Xu, J.; Li, Y.; Chen, L.; Cheng, K.; Liu, G.; Yang, N.; Li, Y.; Nie, G. Biomimetic Metal–Organic Framework Nanoparticles for Cooperative Combination of Antiangiogenesis and Photodynamic Therapy for Enhanced Efficacy. *Adv. Mater.* **2019**, *31*, 1808200. https://doi.org/10.1002/adma.201808200.

149. Haddad, S.; Abánades Lázaro, I.; Fantham, M.; Mishra, A.; Silvestre-Albero, J.; Osterrieth, J. W. M.; Kaminski Schierle, G. S.; Kaminski, C. F.; Forgan, R. S.; Fairen-Jimenez, D. Design of a Functionalized Metal–Organic Framework System for Enhanced Targeted Delivery to Mitochondria. *J. Am. Chem. Soc.* **2020**, *142* , 6661–6674. https://doi.org/10.1021/jacs.0c00188.

150. Yao, J.; Liu, Y.; Wang, J.; Jiang, Q.; She, D.; Guo, H.; Sun, N.; Pang, Z.; Deng, C.; Yang, W.; Shen, S. On-Demand CO Release for Amplification of Chemotherapy by MOF Functionalized Magnetic Carbon Nanoparticles with NIR Irradiation. *Biomaterials* **2019**, *195*, 51–62. https://doi.org/10.1016/j.biomaterials.2018.12.029.

151. Li, X.; Porcel, E.; Menendez-Miranda, M.; Qiu, J.; Yang, X.; Serre, C.; Pastor, A.; Desmaële, D.; Lacombe, S.; Gref, R. Highly Porous Hybrid Metal–Organic Nanoparticles Loaded with Gemcitabine Monophosphate: A Multimodal Approach to Improve Chemo- and Radiotherapy. *ChemMedChem* **2019**, *15*, 274–283. https://doi.org/10.1002/cmdc.201900596.